Transition Rate Enhancement in Reduced Dimensional Optoelectronic Devices

A Thesis

Submitted to the Faculty

of

Drexel University

by

Anushka Bhardwaj

in the partial fulfillment of

requirements for the degree

Of

Master of Science in Electrical Engineering

September 2017

This is to Mom, Dad, Richa,

Abhinav and Keyur for their constant

support during my thesis.

Acknowledgements

I would like to thank Dr. Bahram Nabet for his tireless motivation and continuous guidance. I am grateful to my family for their constant support. I am grateful to Dr. Ioannis Savidis and Dr. James Shackleford for serving in my thesis committee and for their valuable feedback. I would also like to thank Mr. Zhihuan Wang for the valuable discussions during my Research. I am thankful to my friends Rohit and Pawan for their motivation and support.

TABLE OF CONTENTS

LIST OF FIGURES

LIST OF TABLES

Abstract

Junctions of dissimilar semiconductors, heterojunctions, have been used in a variety of electronic, photonic, and optoelectronic devices. A prime example is the invention of Double Heterojunction (DH) lasers by H. Kroemer and Z. Alferov which was awarded the Nobel Prize in Physics in 2000 for "laying the foundation of modern information technology." When the distance between the two heterojunctions is reduced to a few nanometers, electron motion is confined to two dimensions resulting in a Quantum Well (QW). QW lasers which followed DH lasers show much better optoelectronic properties such as higher efficiency, narrower linewidth, and smaller threshold current.

In this thesis, we analyze the effect of dimensionality on the absorption and emission properties of optoelectronic devices. We compare GaAs/AlGaAs DH, Multiple Quantum Well (MQW) and Quantum Wire Lasers where the active region is made of GaAs in each device. Specifically, we calculate the spontaneous emission rate and optical gain of these devices. This analysis helps to determine the underlying physics for the significant increase in the transition rates and optical gain of these devices due to electron confinement. We examine band-to-band optical transition rates for (a) 3D case of DH lasers, (b) 2D case of QW lasers, and (c) 1D case of Quantum wires, and derive and compare, spontaneous emission spectra and the gain coefficient for the three cases. We identify how dimensionality enhances emission spectra through modification of the Joint Optical Density of States (JODS) and oscillator strength. Finally, this study helps explain why heterojunction-based core-shell nanowires show enhanced optoelectronic properties compared to core-only, or homojunction core-shell nanowires.

CHAPTER-1

INTRODUCTION

Semiconductor devices have been used in number of active and passive Optoelectronic devices such as photodetectors, Light Emitting Diodes (LED's), lasers, solar cells, and optical antennas. Properties of semiconductor material change when we move from three-dimensional devices to one-dimensional devices due to change in density of states function, absorption coefficient and joint optical density of states. One-dimensional devices show highest absorption of light as compared to two-dimensional and bulk materials as their absorption coefficient is highest.

1.1.Background and Literature review

This section gives a review of the evolution of Semiconductor lasers and discusses about the motivation for these devices over the time.

1.1.1. Double heterostructures and Multiple quantum wells

Heterojunction were introduced in semiconductor industry at the very dawn of electronics. The motivation to use heterostructures came from the work of H. Kroemer where he assumed that heterojunction may exhibit higher injection efficiencies as compared to homojunctions [1]. On examination of heterostructures, it was found that these structures exhibited (i) optical confinement, (ii) electron confinement and (iii) super injection of carriers which was found to be very beneficial for LED's, solar cells, and photodetector applications [2]. The wide gap window effect in heterostructures allowed to broaden and control the spectral region of solar cells and photodetector and improved efficiency of LED's [2]. Main advantages of Double Heterostructures

(DHS) as low threshold at room temperature DHS lasers [3]. Continuous wave operation of room temperature III-V lasers was first reported in 1970 [4] and is was found that the threshold current density was decreased by a factor of 4 as compared to previous heterostructure lasers. This DHS laser was realized in stripe geometry, depicted by Figure 1-1.

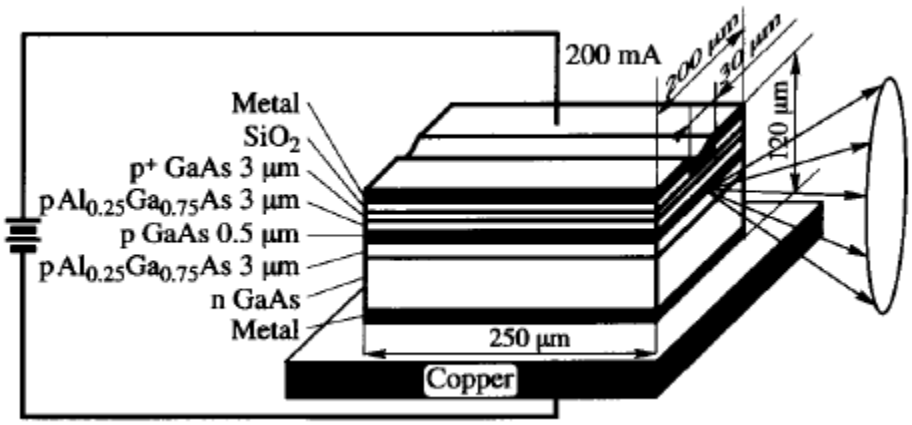

Figure. 1-1. Schematic view of first DHS continuous wave laser.

Although DHS laser offered electron confinement, many experiments lead to the discovery of quantum well lasers where the active region was reduced to some hundred angstroms and the electron level split due to quantum size effect. This effect is known as quantum confinement which occurs when the active region is below the de Broglie wavelength of the active region material of the laser.

The first quantum well laser operation was shown by J.P. van der Ziel et. al in 1975 [5]. Although, the performance of this structure was comparable to a heterostructures and no new properties were observed. In the expectation of lower threshold current, research groups experimented by reducing the dimensions of the device and invented novel structures like quantum wells and multiple quantum wells. The effects in optical properties of a semiconductor device was first depicted with GaAs-AlGaAs heterostructures with a thin layer of GaAs quantum well by Dingle *et al*. [6].

Leading to that, careful examination was made at AT&T Bell laboratories by Miller *et al.* [7] on optical properties of semiconductor quantum wells. The structure of their device is depicted in Figure. 1-2. GaAs/AlGaAs multiple quantum wells of width 96 Angstrom were studied and it was observed that absorption in this structure increases with increasing carrier concentration (Figure. 1-3) [8]. Also, absorption coefficient decreased at low temperature of 75 K as compared to room temperature [9].

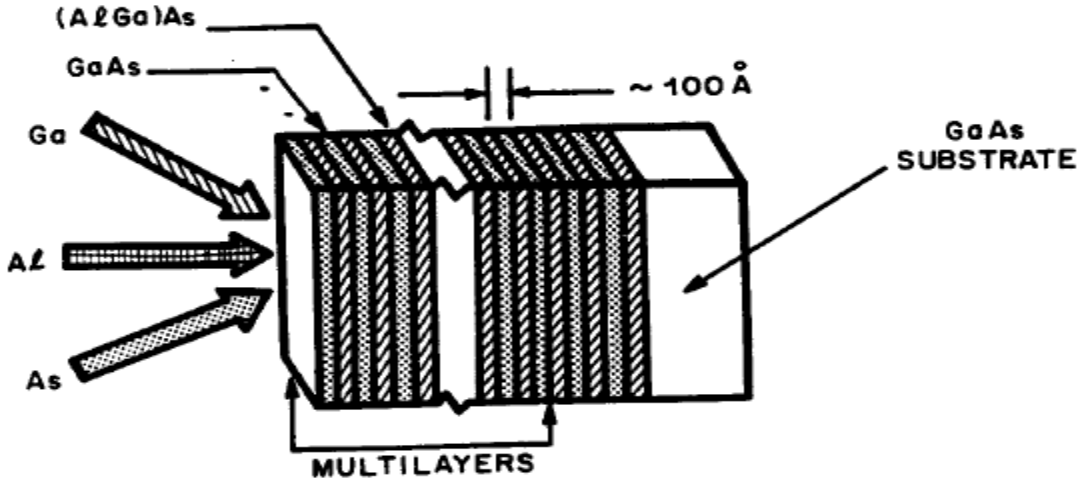

Figure. 1-2. Schematic of Multiple quantum well laser

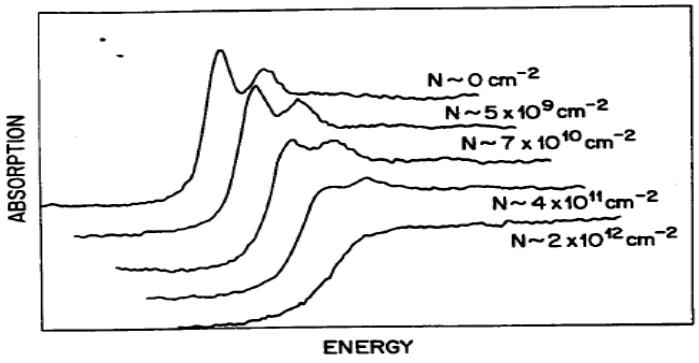

Figure. 1-3. Absorption spectrum of GaAs/AlGaAs multiple quantum well structure (well width = 96 Å) with different carrier concentration; from [5]

The main advantages of quantum wells are their high mobilities and saturation drift velocities and low effective masses which give high confinement energies [10]. Quantum well lasers have

superior performance than bulk lasers due to their low threshold current, high frequency operation capability, narrower linewidth, and low increase of threshold current with temperature [11]. Although, the threshold current is lower than DH lasers but a MWQ laser has a poor optical confinement factor [12-15]. But the decrease in optical confinement factor is compensated by an increase in material gain for a narrower active region. Also, the gain spectra are broader for QW lasers as compared to DH laser [16].

1.1.2. Nanowires

From the above literature review it was observed that quantum wells are better than Double heterostructures in terms of gain and threshold current, but were found to be poor in optical confinement. To solve this problem, scientists discovered novel structure by reducing the dimensions of the device to a few nanometers to find the effect on emission and absorption properties of the device. After quantum wells, they were found to exhibit enhanced efficiency in terms of gain, absorption, and transition rates [17]. They have various applications in optoelectronic devices such as photodetectors [18], LED's [19], solar cells [20] and lasers [21]. These miniaturized one-dimensional structures attracted interests of many scientists when they were found to exhibit lasing action. The first lasing action in a nanowire was observed for a ZnO nanowire in 2001 [21]. In the domain of nanowire lasers, ZnO and GaN have gained popularity due to their low threshold gain and threshold current densities values. In III-V semiconductors, GaAs, AlGaAs and GaN are widely used. Single nanowires have been fabricated and tested for their optical gain and it was found that these nanowires exhibited lowest gain of 250 cm^{-1} for the diameters above 300 nm as compared to bulk GaAs [22]. Absorption in GaAs nanowire with radius

of 20, 30 and 40 nm were compared to GaAs thin film and it was found that nanowires exhibited large absorption as compared to thin films by a factor of 2 [23].

1.2.Project Overview

As per Moore's law, the dimensions of transistors in an integrated circuit have been reduced by a factor of two in every eighteen months. Further scaling down of devices faces limitations in fabrication and device performance. Reduced dimensional structure shows potential to answer this challenge. To analyze the performance of these structure, we study these structures in detail in this thesis. In this thesis, we calculate the optical gain, absorption coefficient, stimulated emission rate, spontaneous emission rate of Double Heterojunction, multiple quantum well and nanowire lasers. We observe that reduced dimensional devises of same volume and lengths leads to improved performance of devices in terms of efficiency, transition rates, absorption coefficient and spontaneous emission rate. Optoelectronic devices have evolved tremendously in the past few decades with discovery of new parameters in these devices. Although a lot of research has been done on emission and gain behavior of lasers but transition rates have been discussed seldom. The motivation of this work came from the desire to contribute to the optoelectronics realm and demonstrate the transition rates in 3-D, 2-D, and 1-D lasers.

It has been observed in various optoelectronic devices that with reduced dimensions, the efficiency of devices increases such as reduction of threshold injection current in quantum well, multiple quantum well and nanowire lasers. It is also observed that the absorption increases with reduction in dimensions of the devices. Hence it is depicted that with help of these devices, enhanced performance can be achieved by devices with minimal consumption of space. The significance of this work is that it gives a clear script of the properties of 3-D, 2-D and 1-D devices which can be used in optoelectronics device development. In this electronics age, it becomes essential for device

engineers to manipulate the device characteristics and parameters, and with the help of this work they can design devices per the required specifications. It will also be of importance, as it will provide guidance in maintaining a trade-off between cost and performance of their devices.

1.3.Outline of Thesis

In chapter 1, we discussed the previous work related to Double Heterojunction, Multiple quantum Well lasers and the evolution of these devices and their optoelectronic properties. This Chapter highlights the overview of this thesis and importance of this work in this era of electronics and optoelectronics devices.

In chapter 2, we start with understanding the basics of optoelectronic devices in order to understand the working of these devices. This chapter discusses the conception of transitions in a two-level energy system, by describing the concepts of absorption and emission in semiconductors and types of transitions are also discussed. Later, the absorption and emission in three-dimensional, two-dimensional, and one-dimensional optoelectronic devices are discussed in detail to understand the functioning of these devices and the effect of dimensionality on emission and absorption properties.

Chapter 3 explains how to estimate the transition rates in nanowires. First, the Joint Optical Density of states in three-dimensional, two-dimensional, and one-dimensional devices are discussed followed by oscillator strength in three-dimensional, and two-dimensional devices. Finally, the effect of dimensionality on these parameters are discussed.

Chapter 4 focusses on Double Heterojunction lasers and its absorption and emission properties. First, the structure used in this chapter is described followed by discussion on phenomenon of lasing. Optical confinement factor and gain threshold of this device is discussed and calculated.

After this, the optical gain and spontaneous emission rate are calculated and their spectral response is generated to understand the role of factors affecting the emission and absorption properties in this type of laser.

Chapter 5 focusses of Multiple quantum well lasers and its absorption and emission properties. First, the structure used in this chapter is described followed by discussion on phenomenon on lasing. Optical confinement factor and gain threshold of this device is discussed and calculated. After this, the optical gain and spontaneous emission rate are calculated and their spectral response is generated to understand the role of factors affecting the emission and absorption properties in this type of laser. The importance of this chapter is that it compares the optical gain and spontaneous emission rate with the Double Heterojunction lasers discussed in chapter 4 to see the effect of dimensionality on the transition rates.

In chapter 6, the Nanowire lasers and their emission and absorption properties are discussed followed by calculation of optical gain, stimulated emission rate and spontaneous emission rate. Also, the spectral response of these parameters is generated. Finally, the spontaneous emission rate and optical gain of nanowire laser are compared with multiple quantum well laser and double heterojunction laser discussed in chapter 5 and chapter 4, respectively.

Finally, the results and conclusions are summarized at the end of this thesis.

CHAPTER 2

EFFECT OF BAND TO BAND EMISSION AND ABSORPTION

2.1. Introduction

Semiconductors are used in various optoelectronic devices such as LED's, Lasers, and solar cells. The transition of carriers between the two energy levels of semiconductors is the basis of working of any optoelectronic devices. The physics and transition of carriers in semiconductors are discussed in detail in this chapter.

2.2. Absorption and emission in semiconductors

The upward and downward transitions of atoms between the energy bands is the foundation of the operation of various optical and optoelectronics devices. Upward and downward transition of atoms results in absorption and emission of light respectively [24]. The intensity of absorption and emission spectra helps in characterization of materials. It also gives information about the direct and indirect transitions and the bad gap of the material and the density of states.

The phenomenon of transition of carrier for lower energy state to upper energy state in presence of excitation field is known as absorption. These transitions are also classified as direct and indirect.

2.2.1 Direct bandgap absorption and emission

In a direct transition, the electron is raised from the top of the valence band to the bottom of the conduction band with no change in momentum. When an electron is dropped without any change in momentum, the phenomenon is called direct emission.

Direct transition occurs from $\varepsilon(k')$ to $\varepsilon(k'')$ as depicted in Figure 2-1, depicting no change in momentum [24].

where,

$$\varepsilon(k') = -\frac{\hbar^2 k'^2}{2m_h^*} \tag{2.1}$$

$$\varepsilon(k'') = E_g + \frac{\hbar^2 k'^2}{2m_e^*} \tag{2.2}$$

where E_g is the direct bandgap at $k = 0$ and m_h^* and m_e^* are the reduced effective mass of holes and electrons in the valence and conduction band respectively.

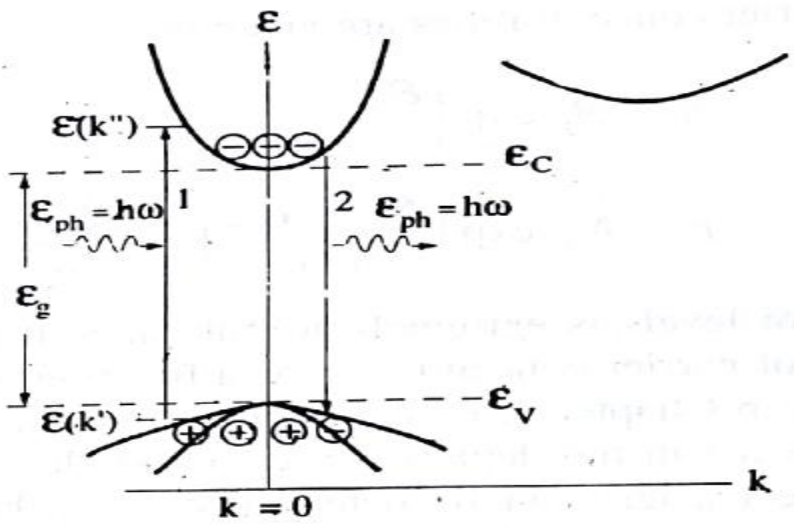

Figure. 2-1. Direct band transitions; from [24]

2.2.2. Indirect bandgap Transitions

In indirect transitions, change of momentum of electron is required. For such transitions, energy and momentum of phonons is required. Although conservation of momentum is required for both direct and indirect transitions. Conservation of momentum requires:

$$k'' + k_p = k' + k_{ph} \tag{2.3}$$

where k_p is the wavevector of the phonon and k_{ph} is the wavevector of the absorbed phonon. Since the k_{ph} is small, so the conservation of momentum for an indirect transition is given by:

$$k'' - k' = +k_p \tag{2.4}$$

Indirect transition can be understood by radiative and non-radiative recombination. Non-radiative recombination is where carriers recombine without the absorption and emission of photons, but involves emission and absorption of phonons. On the other hand, radiative recombination is a process is where the carriers recombine and emit photons.

2.2.2.1. Indirect Absorption

Indirect band Absorption can be explained with the help of Figure 2-2. In this transition, the conduction band minimum is not at k = 0 therefore the transition requires the change in momentum which is facilitated by involvement of phonons. Thus, the electron siting in the conduction band minima at k≠0 cannot combine with the hole at k = 0 until a phonon with the required energy and k vector is available to initiate the transition. The dwelling time of the electron in conduction band minima increases depending on the availability of the phonon with right amount of energy. The energy required for upward transition is ε_{ph} which is equal to $\varepsilon_g + \varepsilon_p$ where ε_g and ε_p is the band gap energy and energy of phonon respectively. These transitions take place when a phonon with the right amount of energy is absorbed and the total amount of energy for the transition is equal to the energy band gap energy plus energy of phonon.

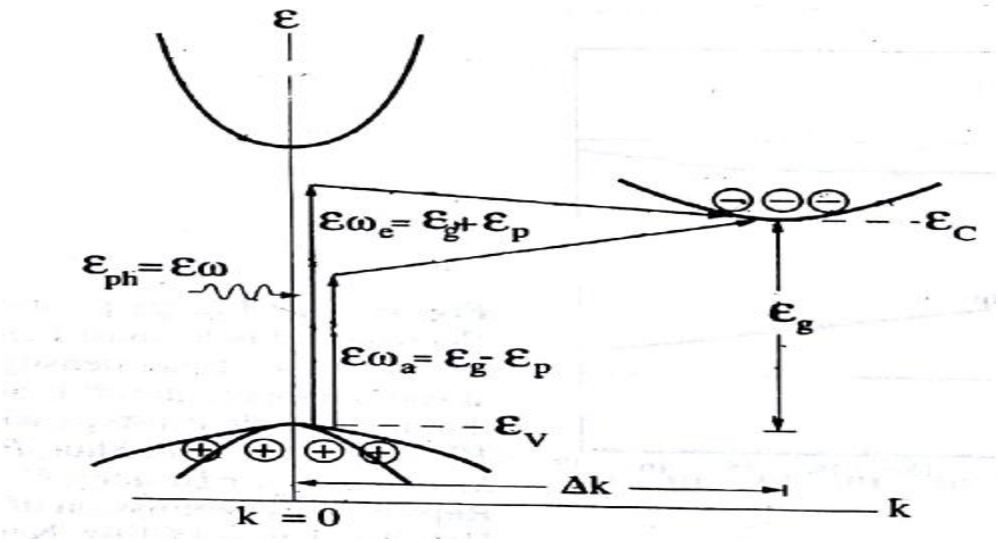

Figure. 2-2. Indirect band Absorption; from [24]

2.2.2.2. Indirect Emission

Indirect band emission can be explained with the help of Figure. 2-3 where the emission results in emission of phonon and photon. The energy of photon is given by ε_{ph} which is equal to $\varepsilon_g - \varepsilon_p$, where ε_g and ε_p is the band gap energy and energy of phonon respectively.

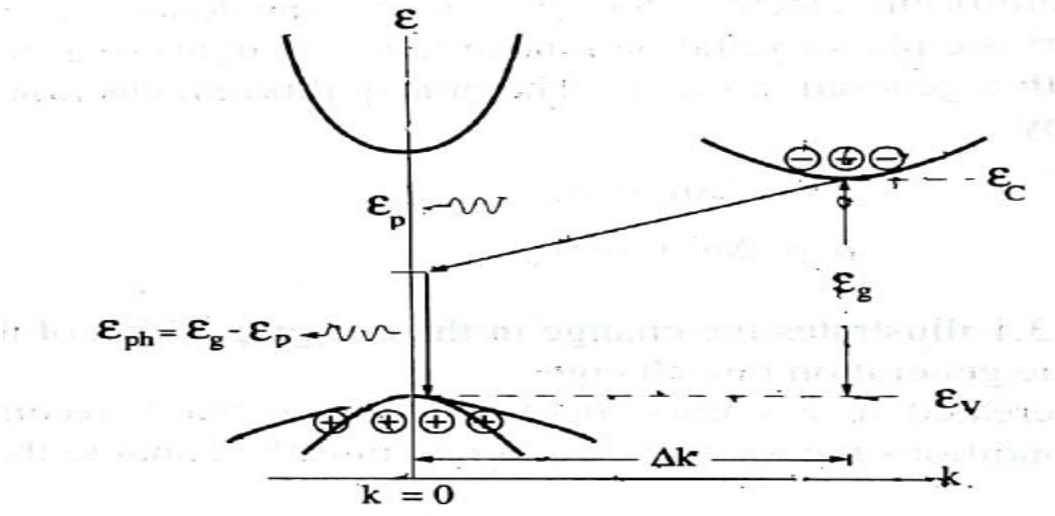

Figure. 2-3. Indirect Band Emission; from [24]

Where $\Delta k = k_p$

2.3 Effect of dimensionality on band-to-band emission and absorption

Study of band to band optical transitions in a semiconductor is an important aspect in optical and optoelectronic devices such as photodetectors, LED's, solar cells, and lasers. The band to band optical transitions are described by stimulated, spontaneous emission rates and stimulated absorption rates. These rates are dependent on various parameters such as momentum matrix element and joint optical density of states. These rates change from one-dimensional structures to three-dimensional structures as the joint optical density of states and momentum matrix element are dimension-dependent quantities. In this chapter, we study the change of the rates with dimension of the structure and how can we quantify the effect of dimensions on transition rates in semiconductors. With the determination of transition rates, it can be determined that what kind of a structure is best suited for a certain application.

2.3.1. Absorption and Emission in bulk semiconductor

To study the effect of dimension on band to band optical transitions, we study the transition rates for absorption and emission from valence band to conduction band. The key parameters that play an important role in transition rate are momentum matrix element and joint optical density of states, which will be discussed in this chapter.

The interaction between electrons and photon can be described by the Hamiltonian as given below [25]

$$H = \frac{1}{2m_0}(p - eA)^2 + V(r) \tag{2.5}$$

where A is the vector potential representing electromagnetic field and $V(r)$ is the periodic crystal potential, p is the momentum variable and r is the position vector. The expansion of the Hamiltonian results in:

$$H = \frac{p^2}{2m_0} + V(r) - \frac{e}{2m_0}(p.A + A.p) + \frac{e^2A^2}{2m_0} \tag{2.6}$$

$$\cong H_0 + H'$$

where H_0 is the unperturbed part of the Hamiltonian and H' is the perturbation caused by the light. The perturbed and unperturbed Hamiltonian can be written as:

$$H_0 = \frac{p^2}{2m_0} + V(r) \tag{2.7}$$

$$H' = -\frac{e}{m_0}(A.p) \tag{2.8}$$

From Coulomb Gauge rule, we know that

$$\nabla.A = 0 \tag{2.9}$$

such that $p.A = A.p$ and$p = (\hbar/i)\nabla$, with the term $\frac{e^2A^2}{2m_0}$ in equation (2.6) being much smaller than A and thus can be ignored.

Using Fermi's Golden rule, the rate of upward transition can be derived. The Fermi's Golden rule is given by:

$$W_{if} = \frac{2\pi}{\hbar}|H'_{fi}|^2 \ \delta(E_f - E_i - \hbar\omega) + \frac{2\pi}{\hbar}|H'_{fi}|^2 \ \delta(E_f - E_i + \hbar\omega), \tag{2.10}$$

i and f represents the initial and final states in a semiconductor and the momentum matrix element H'_{fi} is given by:

$$H'_{fi} = -\frac{e}{m_0} A. < f|p|i > = \frac{eA_0}{2m_0}.\hat{n}.\ p_{fi} \tag{2.11}$$

If the electron is in state i (also valence band) and $E_c > E_v$ then the transition rate from valence band to conduction band which is given by

$$W_{\uparrow}(k_i) = \frac{2\pi}{\hbar} |\langle f|H'(r))|i\rangle|^2\ \delta(E_C(k_i) - E_V(k_i) - \hbar\omega) \tag{2.12}$$

this can be written as

$$W_{\uparrow}(k_i) = \frac{2\pi}{\hbar}\left(\frac{qA_0}{2m}\right)^2 |\hat{n}.\ p_{cv}|^2\ \ \delta(E_C(k_i) - E_V(k_i) - \hbar\omega) \tag{2.13}$$

where, p_{cv} is the interband momentum matrix element, the delta function represents the energy conservation and *m* is the mass of the electron.

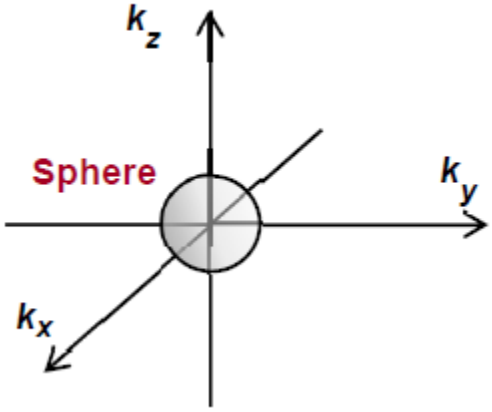

Figure. 2-4. K-space in a bulk semiconductor.

Here we are interested in number of transitions happening per unit volume per second. As can be seen in Figure. 2-4 that the carrier distribution is symmetric in k-space in bulk semiconductor, therefore we take transitions per unit per volume. The upward rate per unit volume per is obtained by summing all the initial states per unit volume and multiplying it by the probability of occupation

of the initial state and the probability that the final state is unoccupied. Therefore, the total upward transition rate is given by [26-29]:

$$R_{\uparrow}(\omega) = \frac{2}{V} \times \sum_{k_i} W_{\uparrow}(k_i)\, f_V(k_i)[1 - f_C(k_i)] \tag{2.14}$$

where, $f_V(k_i)$ is the occupation probability of the valence band and $[1 - f_C(k_i)]$ is the probability of the conduction band being empty.

Assuming the case where conduction band is empty and the valence band is full. So, equation (2.14) reduces to

$$R_{\uparrow}(\omega) \approx \frac{2}{V} \times \sum_{k_i} W_{\uparrow}(k_i) \tag{2.15}$$

$$R_{\uparrow}(\omega) = \frac{2}{V} \times \sum_{k_i} \frac{2\pi}{\hbar}\left(\frac{qA_0}{2m}\right)^2 |\hat{n}.\ p_{cv}|^2\ \ \delta(E_C(k_i) - E_V(k_i) - \hbar\omega) \tag{2.16}$$

$$= 2\times \int \frac{d^3\, k_i}{(2\pi)^3} \frac{2\pi}{\hbar}\left(\frac{qA_0}{2m}\right)^2 |\hat{n}.\ p_{cv}|^2\ \ \delta(E_C(k_i) - E_V(k_i) - \hbar\omega) \tag{2.17}$$

$$= \frac{2\pi}{\hbar}\left(\frac{qA_0}{2m}\right)^2 \langle|\hat{n}.\ p_{cv}|^2\rangle\, 2\times \int \frac{d^3\, k_i}{(2\pi)^3}\ \delta(E_C(k_i) - E_V(k_i) - \hbar\omega) \tag{2.18}$$

$$= \frac{2\pi}{\hbar}\left(\frac{qA_0}{2m}\right)^2 \langle|\hat{n}.\ p_{cv}|^2\rangle\, 2\times \int \frac{d^3\, k}{(2\pi)^3}\ \delta(E_C(k) - E_V(k) - \hbar\omega) \tag{2.19}$$

where the delta function represents energy conservation.

The integral $\int \frac{d^3\, k}{(2\pi)^3}$ represents the joint optical density of states and in the case of bulk (3-D) is given by:

$$\frac{1}{2\pi^2}\left(\frac{2m_r}{\hbar^2}\right)^{3/2} \sqrt{\hbar\omega - E_G}$$

where m_r is the reduced effective mass and E_G is the band gap and $\hbar\omega$ is the energy of photon. Substituting the value of joint optical density of states in the above equation, the total transition rate or absorption rate can be given by:

$$R_{\uparrow}(\omega) \quad = \frac{2\pi}{\hbar}\left(\frac{qA_0}{2m}\right)^2 \langle|\hat{n}.\ p_{cv}|^2\rangle \frac{1}{2\pi^2}\left(\frac{2m_r}{\hbar^2}\right)^{3/2} \sqrt{\hbar\omega - E_G} \tag{2.20}$$

$R_{\uparrow}(\omega)$can also be written in terms of optical intensity I and photon density n_p:

Photon density is defined as number of photons per unit volume, and for a plane wave it is defined by [26-29]:

$$n_p = \frac{Photon\ flow\ per\ unit\ area\ per\ second}{velocity\ of\ photons} \tag{2.21}$$

In other words,

$$n_p = \frac{1}{2}\frac{\omega^2}{\hbar\boldsymbol{\omega}}\ nn_g^M \varepsilon_0 |A_0|^2 \tag{2.22}$$

Power flow per unit area is called the optical intensity and is defined as:

$$I = \frac{n\omega^2}{2\mu_0 c}|A_0|^2 \tag{2.23}$$

By substituting the equation (2.23) and (2.22) in equation (2.20), the total upward transition rate or stimulated absorption rate can be derived as:

$$R_{\uparrow}(\omega) \quad = \left(\frac{q}{m}\right)^2 \left(\frac{\pi n_p}{\omega\ nn_g^M \varepsilon_0}\right) \langle|\hat{n}.\ p_{cv}|^2\rangle \frac{1}{2\pi^2}\left(\frac{2m_r}{\hbar^2}\right)^{3/2} \sqrt{\hbar\omega - E_G} \tag{2.24}$$

2.3.1.1. Stimulated Emission

The stimulated emission also can be calculated using Fermi's Golden rule and can be obtained using the same procedure that was adopted to calculate the stimulated absorption in semiconductor. The stimulated emission rate is given by [26-29]:

$$R_{\downarrow}(\omega) = \left(\frac{q}{m}\right)^2 \left(\frac{\pi n_p}{\omega\, n n_g^M \varepsilon_0}\right) \langle|\hat{n}.\ p_{cv}|^2\rangle\ 2\times \int \frac{d^3\,k}{(2\pi)^3}\ f_C(k)[1-f_V(k)]\ \delta(E_C(k)-E_V(k)-\hbar\omega) \tag{2.25}$$

2.3.1.2. Momentum matrix element for bulk semiconductor

The momentum matrix element in a bulk semiconductor is given by:

$$\langle|\hat{n}.\ p_{cv}|^2\rangle = \frac{mE_p}{6} \tag{2.26}$$

where the energy E_p is dependent on the type of material. For example, E_p=25.7 for GaAs at 300 K.

2.3.2. Absorption and Emission in Quantum Well

In this section, we will examine how optically induced transitions change when the system becomes reduced dimensional. Figure. 2-5 depicts the energy level in a quantum well. In a quantum well the quantum confinement occurs as the dimensions of a quantum well is less than De Broglie wavelength. As depicted in Figure. 2-5, the conduction and valence band have discrete energy levels $E_1^c, E_2^c and\ E_1^v$ which corresponds to quantum numbers in conduction and valence band and L is the width of the quantum well.

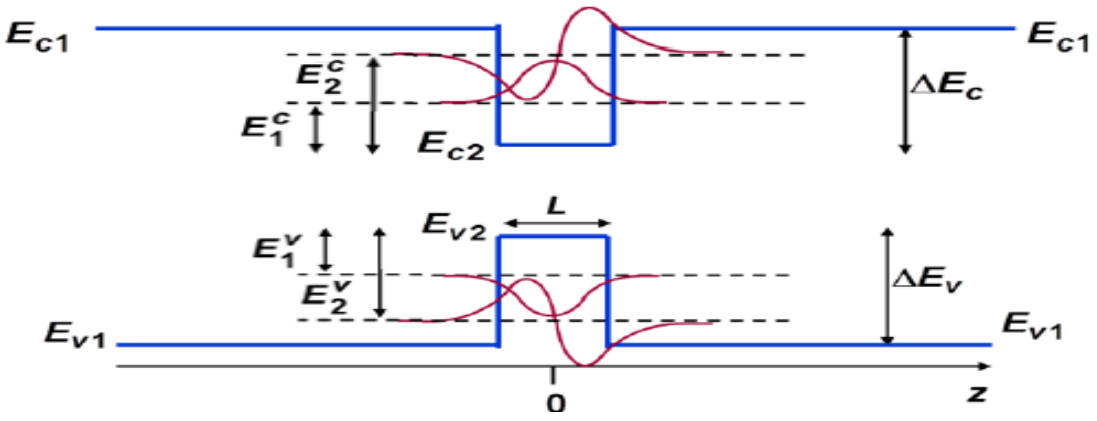

Figure. 2-5. Energy band levels in a quantum well.

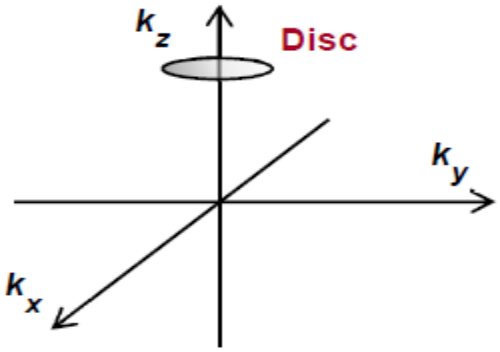

Figure. 2-6. K-space in a quantum well.

2.3.2.1. Stimulated absorption and stimulated emission in quantum well

The band to band (interband) transition rates in a quantum well can be determined using Fermi's Golden rule as described for the bulk case. However, as it can be seen in Figure. 2-6 that the carrier distribution is asymmetric in k-space for a quantum well and the energy and momentum is quantized in z direction, therefore we take transitions per unit area per second in a 2-D case. And

the spontaneous absorption rate is the upward transitions per unit area per second which is given by:

$$R_{\uparrow}(s,p,\omega) = \left(\frac{q}{m}\right)^2 \left(\frac{\pi n_p}{\omega\, n n_g^M \varepsilon_0}\right) \left|\int dz [\Phi_s^c(z)]^* \Phi_p^V(z)\right|^2 \times 2 \times$$

$$\int \frac{d^2 k_{||}}{(2\pi)^2} |\hat{n}.\ p_{cv}(k_0, k_0')|^2 f_V(p, k_{||})[1 - f_C(s, k_{||})]\ \delta(E_C(s, k_{||}) - E_V(p, k_{||}) - \hbar\omega) \qquad (2.27)$$

and stimulated emission is downward transitions per unit area per second, and is given by [26-29]:

$$R_{\downarrow}(s,p,\omega) = \left(\frac{q}{m}\right)^2 \left(\frac{\pi n_p}{\omega\, n n_g^M \varepsilon_0}\right) \left|\int dz [\Phi_s^c(z)]^* \Phi_p^V(z)\right|^2 \times 2 \times$$

$$\int \frac{d^2 k_{||}}{(2\pi)^2} |\hat{n}.\ p_{cv}(k_0, k_0')|^2 f_C(s, k_{||})[1 - f_V(p, k_{||})]\ \delta(E_C(s, k_{||}) - E_V(p, k_{||}) - \hbar\omega) \qquad (2.28)$$

for conduction bands s=1,2,3 and for valence band p=1,2,3. Where k_0 wavevector is the function of transverse wavevector $k_{||}$ and k_0 is nearly parallel to the z-axis, and the integral represents the joint density of states in a quantum well.

2.3.2.2. Momentum matrix element in a quantum well

In a quantum well, the momentum matrix element is given by:

$$\langle|\hat{n}.\ p_{cv}(k_o, k_o')|^2\rangle = \frac{mE_p}{4}(n_x^2 + n_y^2) \qquad (2.29)$$

where n_x and n_y are the quantum numbers.

Findings

As it can be seen from the above derived expression for stimulated absorption rate and stimulated emission rate that the emission and absorption is the dependent on the momentum matrix element

and joint optical density of states for a bulk semiconductor and a quantum well case. As it can be seen, that for the bulk semiconductor the momentum matrix element is $\frac{mE_p}{6}$ (equation 2.26) and comparing it with momentum matrix element of quantum well, which is given by equation 2.29, we see that momentum matrix element in bulk case is lower than the momentum matrix element of quantum well by a factor of (0.09). We know that joint optical density of states in a bulk semiconductor is given by $N(J)_{2D} = \frac{1}{2\pi^2}(\frac{2m_r}{\hbar^2})^{3/2}\sqrt{\hbar\omega - E_G}$ and for a quantum well it is given by $N(J)_{2D} = \frac{m_r}{\pi\hbar^2 L}$.

Where the joint optical density of states will vary from 2-D to 3-D due to energy dependence in 3D and the reduced effective mass. The reduced mass is given by $\frac{1}{m_r} = \frac{1}{m_e} + \frac{1}{m_h}$ is dependent on effective mass of holes and electrons. From the above expression, we can deduce that the reduced mass is higher in a bulk semiconductor as compared to quantum wells as $m_h = 0.51m_0$ for bulk GaAs [36] and $m_{hh} = 0.118m_0$ in GaAs quantum wells [35]. Therefore, reduced mass m_r=0.055m$_o$ for bulk GaAs and m_r=0.041m$_0$ for GaAs in a quantum well.

Comparing the joint optical density and taking the effect of reduced mass in account the reduced mass in bulk semiconductor is lower by the factor of 0.023 as compared to reduced effective mass in quantum well, where we took GaAs as an example. This tells us about the change of factor in joint optical density of states from 2-D to 3-D and hence the change in absorption and emission rates for 2-D and 3-D structures.

From the above findings, we can conclude the effect of dimensions on the band to band optical absorption and emission in semiconductors and by what factor absorption and emission will vary from 3-D to 2-D

CHAPTER 3

TRANSITION RATES IN QUANTUM WIRES

3.1. Introduction

Transition rates is a function of Joint Optical Density of states (JODS) and oscillator strength in optoelectronic devices. In this chapter, we discuss the estimation of effect of JODS and oscillator strength on transition rates in quantum wires. This effect is also discussed for bulk and quantum Well devices in this chapter.

3.2. Joint Optical Density of States

Conservation of momentum and energy forces the photon to interact with electrons and holes of specific momentum and energy. This interaction is described Joint Optical Density of states, $N_J(\varepsilon)$. The electronic density of states is related to JODS by:

$$N_J(\varepsilon) = \frac{m_r}{m_e} N(\varepsilon_2) \tag{3.1}$$

where $N(\varepsilon_2)$ is the electronic density of states.

The joint optical density of states for a bulk semiconductor is given by [25]:

$$N_J(\varepsilon)^{3D} = \frac{1}{2\pi^2}\left(\frac{2m_r}{\hbar^2}\right)^{3/2} \sqrt{E - E_G} \tag{3.2}$$

where E= ħω i.e the energy of the photon.

The joint optical density of states for a quantum well can be described as [25]:

$$N_J(\varepsilon)^{2D} = \frac{m_r}{\pi\hbar^2 L} \tag{3.3}$$

where m_r is the reduced effective mass and L is the width of the quantum well.

The joint optical density of states for a rectangular quantum wire is [25]:

$$N_J(\varepsilon)^{1D} = \frac{1}{L_x L_y \pi}\sqrt{\frac{2m_r}{\hbar^2}}\ \frac{1}{\sqrt{\hbar\omega - E_{cv}^{mn}}} \tag{3.4}$$

where,

$$E_{cv}^{mn} = E_g + \frac{\hbar^2}{2m_r}\left[\left(\frac{m\pi}{a}\right)^2 + \left(\frac{n\pi}{b}\right)^2\right] \tag{3.5}$$

Here E_g is the band gap of the material, L_x and L_y is the width of the nanowire, m and n are the quantum numbers and a x b is the cross section of the quantum wire.

Joint optical density of states is thus seen to be dependent on reduced effective m_r, where

$$\frac{1}{m_r} = \frac{1}{m_e} + \frac{1}{m_h} \tag{3.6}$$

where m_e is the effective mass of the electron and m_h is the effective mass of the holes.

In quantum wells and quantum wires the m_{hh} is effective mass for heavy hole in the first valence subband and m_{lh} is the effective mass of light hole in the second valence subband. Effective mass is conduction band and valence band depends on the type of material. By comparison of effective mass for GaAs/AlGaAs quantum wire and quantum well for heavy hole it was found that that $m_{hh}$for quantum wire was 0.027 m_0 and m_{hh} for quantum well was 0.118m_0 [35], where m_0 = $9.10938356 \times 10^{-31}$ kg.

From the above discussion, we can observe that the reduced effective mass is lower for quantum wires and higher in quantum well, because of the values compared from equation (3.6) for quantum wells and quantum wires. Hence, the Joint optical density of states will change according to the reduced effective mass.

3.3. Oscillator strength

Oscillator strength is the probability of absorption and emission of electromagnetic wave in transitions between the ground state and excited state. The oscillator strength can be thought of as the ratio between the quantum mechanical transition rate and the classical absorption/emission rate of a single electron oscillator with the same frequency as the transition [30-32].

3.3.1. Quantum well

The oscillator strength in a quantum well for optical transition for an exciton state n is given by [33]:

$$f_n = \frac{2}{m\hbar\omega} \left|P_{n,0}\right|^2 \tag{3.7}$$

where m is the mass of the electron, $\hbar\omega$ is the energy of the photon and transition matrix element is described by [33]:

$$P_{n,0} = \sum_q M_{CV}(q,k) A^n\,(q+k,-q) \tag{3.8}$$

where M_{CV} is the matrix element for optical transitions between valence band and conduction band and k is the photon wavevector and $A^n\,(q1,q2)$ is Fourier transform of the exciton wave function.

3.3.2. Quantum wire

The oscillator strength per unit length in quantum wire is given by [34]:

$$f_0 = \frac{2}{m\hbar\omega} |M_{cv}^{ex}|^2 \tag{3.9}$$

where

$$|M_{cv}^{ex}|^2 = \left|\frac{1}{2\pi}\int dk_{||}\, \Phi_{eh}(k_|) M_{cv}(k_|)\right|^2 \tag{3.10}$$

where $|M_{cv}^{ex}|^2$ is the momentum matrix element for excitons and M_{cv} is the momentum matrix element for the optical transition between the valence band and the conduction band where the integral represents the joint optical density of states [34].

Findings

From the equation (3.10), we can see momentum matrix element depends on the Joint optical density of states which depends on the reduced effective mass and looking at dependence of oscillator strength on the reduced mass we can deduce that the oscillator strength increases with reduction in reduced mass and reduced mass is lower in quantum wires as compared to quantum well and thus the oscillator strength is reduced in quantum wire structure as compared to quantum wells. The momentum matrix element also describes the dependence of polarization on the incident photonic flux.

3.4. Overlap Integral

3.4.1. Quantum well

In a quantum well the block wave functions for a hole in the valence subband m,

are derived as [25]:

$$\psi_a(r) = u_V(r)\frac{e^{ik_t\cdot\rho}}{\sqrt{A}}\, g_m(z) \tag{3.11}$$

And for an electron in the conduction subband n,

$$\psi_b(r) = u_C(r)\frac{e^{ik'_t\cdot\rho}}{\sqrt{A}}\, \Phi_n(z) \tag{3.12}$$

where $u_V(r)$ and $u_C(r)$ are the periodic parts of the Bloch wave function , A is the area of the quantum well and the transverse wavevectors $k_t = k_x\hat{x} + k_y\hat{y}$, $k'_t = k'_x\,\hat{x} + k'_y\hat{y}$ and the position vector $\rho = x\hat{x} + y\hat{y}$.

And the overlap integral is defined by [25]:

$$I_{hm}^{en} = \int_{-\infty}^{+\infty} dz \Phi_n^* \, g_m(z) \tag{3.13}$$

3.4.2. Quantum wire

The Bloch wave function in a rectangular quantum wire is given by [25]

$$\psi_c = \frac{2}{\sqrt{ab}} \, sin\left(\frac{m\pi x}{a}\right) sin\left(\frac{n\pi y}{b}\right) u_c(r) \frac{e^{ik_z.z}}{\sqrt{L}} \tag{3.14}$$

for conduction band and,

$$\psi_V = \frac{2}{\sqrt{ab}} \, sin\left(\frac{m'\pi x}{a}\right) sin\left(\frac{n'\pi y}{b}\right) u_V(r) \frac{e^{ik'_z.z}}{\sqrt{L}} \tag{3.15}$$

for the valence band, where a×b is the cross section of the wire and L is the length of the wire and the overlap function is given by the integral of electron and hole envelope function.

Findings

The overlap integral also expresses the energy dependence of the matrix element for each transition occurring along the length of the nanowires. The overlap integral changes from 2-D to 1-D system as the electron distribution in a 2-D system is attributed to two dimensions in k-space whereas in 1-D system the overlap integral with its envelope functions are taken into consideration along z-axis in k space that is along the length of wire.

3.5. Conclusion

It was found that the stimulated absorption and stimulated emission rate depends on the momentum matrix elements and joint optical density of states. It was found that joint optical density of states and momentum matrix element changed from one-dimensional structures to three-dimensional structures. Joint optical density of states was found to be a function of reduced effective mass which changed from one-dimensional structures to three-dimensional structures. The change in oscillator strength was also studied and it was found that oscillator strength increased with decrease in device dimensions.

CHAPTER 4

DOUBLE HETEROJUNCTION LASER

4.1 Introduction

A Double Heterojunction or Double Heterostructure is formed when one semiconductor material is sandwiched between two other semiconductor materials. The outer layer semiconductor is called the cladding layer. The inner layer in a double heterostructure has a smaller bandgap than the cladding layer.

Energy discontinuities occur at the boundaries in the smaller bandgap material which leads to quantum confinement in the smaller bandgap material. Recombination of electrons and holes takes place in the smaller band gap semiconductor and emission of photons takes place. In this chapter, the design of the heterostructure is described by Figure 4-1, where the active region id made of GaAs and has a width of 1 micrometer. The cladding layer are made of doped AlGaAs.

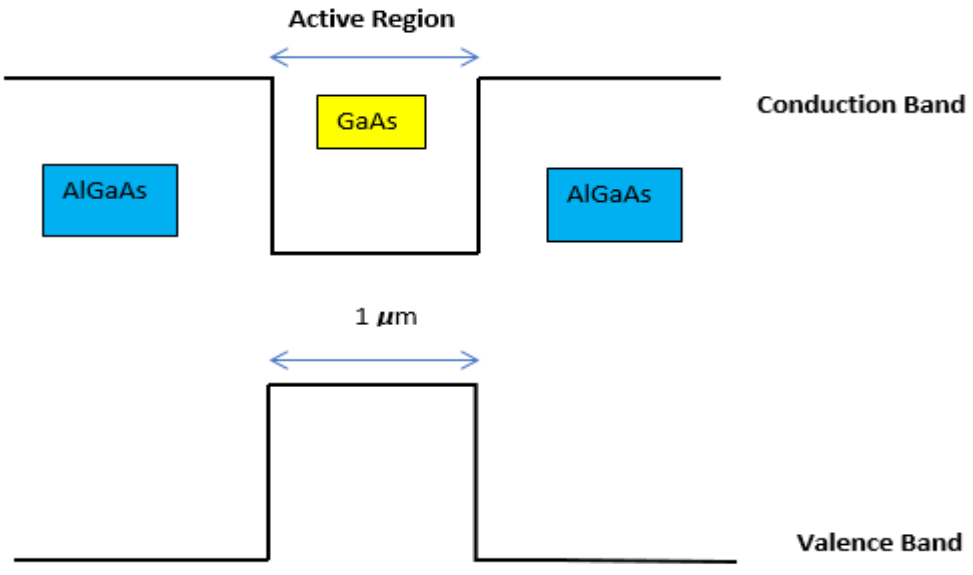

Figure. 4-1. Structure of Double Heterostructure Laser

4.2 Laser Operation

A laser works on the principle of population inversion. Population inversion occurs when most of the atoms or particles in a system are in higher excited states than in lower, unexcited states.

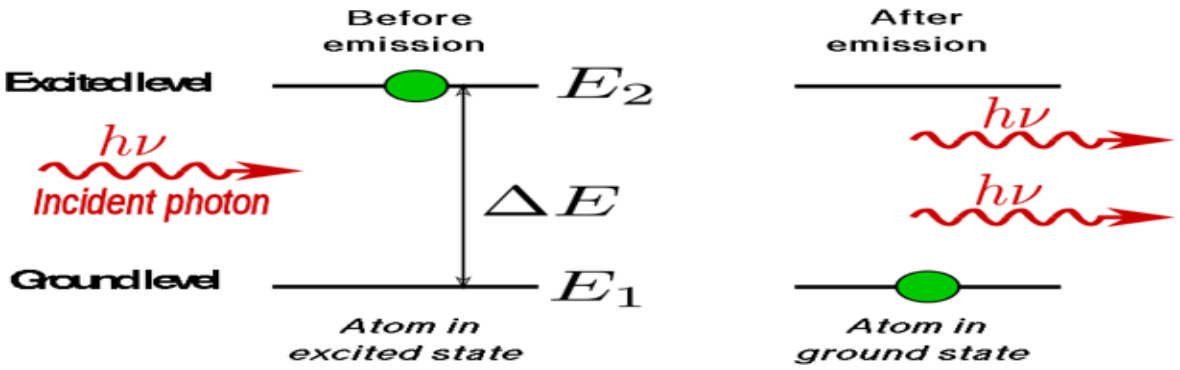

Figure. 4-2. Population Inversion in a two-level system.

Next, we study about optical confinement factor which is an important parameter for laser operation. Optical confinement factor is the measure of modal confinement or the fraction of optical intensity in the active region and is a strong function of the active region thickness.

Optical confinement factor for a Double heterojunction laser is given by [24]:

$$\Gamma = \int_{-d/2}^{d/2} \Psi_m^2 (x) dx \tag{4.1}$$

where d is the thickness of active region and Ψ_m is the photon wave for bulk semiconductor materials.

4.3 Gain in the active region

The optical gain is equal to the net stimulated emission rate divided by the photon flux, that is:

$$g(\varepsilon) = \frac{power\ emitted\ per\ unit\ volume}{power\ crossing\ per\ unit\ area} \tag{4.2}$$

In other words,

$$g(\varepsilon) = \frac{r_{st}^{net}(\varepsilon)}{\frac{c.n_\varepsilon u_\varepsilon}{n_r}} \quad (cm)^{-1} \tag{4.3}$$

where n_ε is the photon mode density, u_ε is the photon occupation number. In the above equation $r_{st}^{net}(\varepsilon)$ is derived as [24]:

$$r_{st}^{net}(\varepsilon) = r_{st}(\varepsilon) - r_{abs}(\varepsilon) \tag{4.4}$$

where $r_{st}(\varepsilon)$ and $r_{abs}(\varepsilon)$ are stimulated emission rate and absorption rate, respectively. Now, net stimulated emission rate can be derived as:

$$r_{st}^{net}(\varepsilon) = (\frac{n_r\, q^2 \varepsilon\, p_{cv}^2 u_\varepsilon}{3\pi\epsilon_0 m_0^2 \hbar^2 c^3}) N_J(\varepsilon)[f_n(\varepsilon_2) - f_p(\varepsilon_1)] \tag{4.5}$$

Here, the first term in the set of parentheses is the stimulated transition probability, $N_J(\varepsilon)$ is the Joint Optical Density of states, $f_n(\varepsilon_2)$ and $f_p(\varepsilon_1)$ are distribution functions for electron and holes in conduction and valence band and are given by [24]:

$$f_p(\varepsilon_1) = exp\left(\frac{\varepsilon - \varepsilon_{fp}}{K_B T}\right) \tag{4.6}$$

$$f_n(\varepsilon_2) = exp\left(\frac{\varepsilon_{fn} - \varepsilon}{K_B T}\right), \tag{4.7}$$

where ε_{fp} and ε_{fn} are quasi fermi levels in valence and conduction band respectively.

$N_J(\varepsilon)$ in equation (4.5) is the Joint optical density of states for bulk semiconductor and is given by [24]:

$$N_J(\varepsilon) = \frac{(2m_r)^{3/2}}{2\pi\hbar^3}\left(\varepsilon - \varepsilon_g\right)^{1/2} \quad (eV^{-1}.cm^{-3}) \tag{4.8}$$

A double heterojunction laser is a three-dimensional structure. Therefore, the Joint optical density of states in the above equation is a three-dimensional JODS for a double heterojunction laser.

After substituting equation (4.5) and (4.8) in equation (4.3) the gain spectra can be expressed as:

$$g(\varepsilon) = \frac{\sqrt{2}(m_r)^{3/2} q^2 p_{cv}^2}{3\pi n_r \in_0 m_0^2 \hbar^2 c\varepsilon} \left(\varepsilon - \varepsilon_g\right)^{1/2} [f_n(\varepsilon_2) - f_p(\varepsilon_1)] \tag{4.9}$$

It can be observed from the above equation that the optical gain is directly dependent on reduced effective mass, occupation probability in conduction and valence band, band gap of the active region material and oscillator strength of the active region material. The expression for the gain spectra is of high significance for laser design, as it is used to find the threshold carrier concentration of the laser by marking the threshold gain value in the spectral response of the optical gain and looking for the corresponding carrier concentration. Plotting equation (4.9), we get gain spectra of DH lasers as follows:

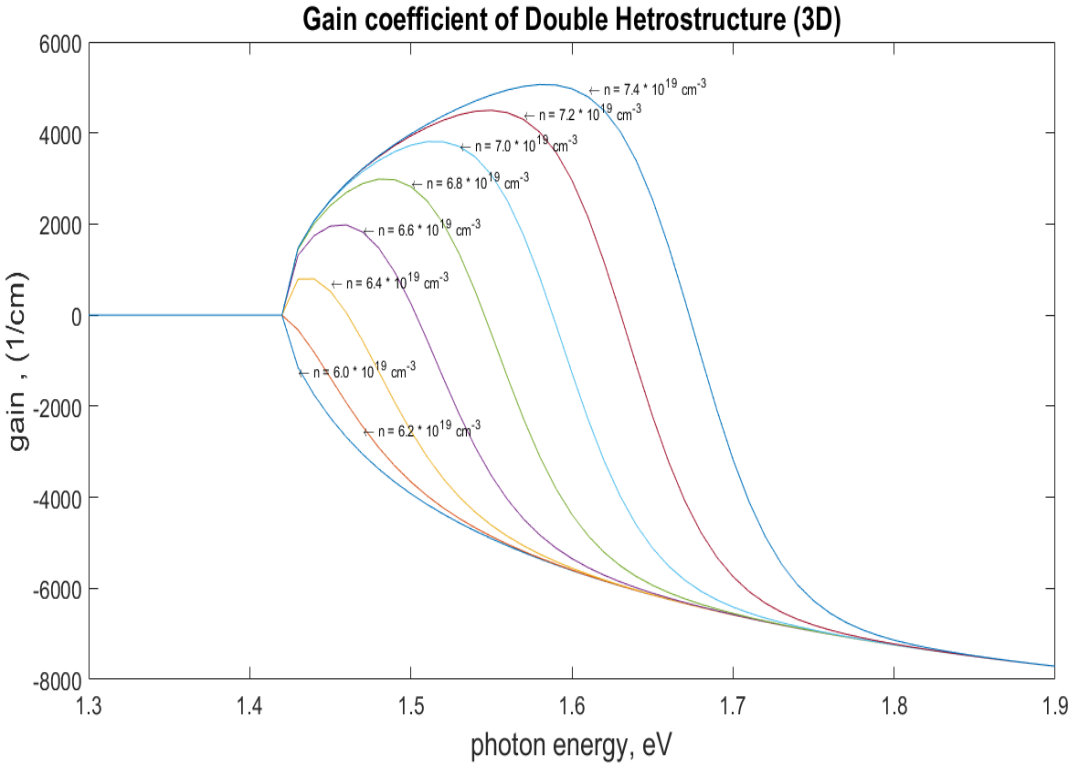

Figure. 4-3. Gain Spectra of Double Heterojunction Laser

The shape of the above gain spectra is because of the 3D JODS and gain coefficient increases as the carrier concentration (n) increases as shown in Figure. 4-3.

4.4. Spontaneous Emission Rate

Spontaneous emission is a process in which the electron or charge carrier in the excited state makes a transition to an unexcited state (ground level) with an emission of photons. This kind of phenomenon is observed in optoelectronic devices such as lasers and LEDs.

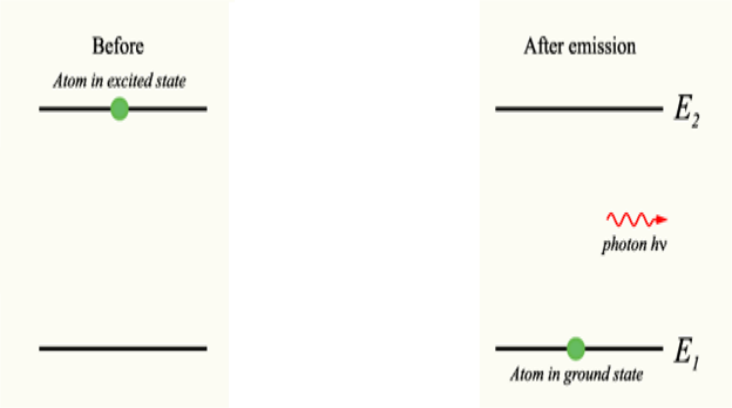

Figure. 4-4. Spontaneous Emission in a two-level system

In a double heterojunction laser, the spontaneous emission rate is given as follow [24]:

$$r_{sp}(\varepsilon) = P_{em}\, N_J(\varepsilon) f_n(\varepsilon_2)\left[1 - f_p(\varepsilon_1)\right] \quad (s^{-1}(eV)^{-1}cm^{-3}) \tag{4.10}$$

where P_{em} is the emission probability and is equal to $P_{em} = \frac{n_r q^2 \varepsilon p_{cv}^2 (1+u_\varepsilon)}{3\pi\varepsilon_0 m_0^2 \hbar^2 c^3}$, where u_ε is the number of photons per mode is equal to unity for spontaneous emission and p_{cv} is the oscillator strength (see Appendix 1).

It is depicted that the spontaneous emission rate is dependent on Joint optical density of states which is dimensional dependent parameter. For bulk devices (3-D devices) Joint optical density of states is given as [24]:

$$N_J(\varepsilon) = \frac{(2m_r)^{3/2}}{2\pi\hbar^3}\left(\varepsilon - \varepsilon_g\right)^{1/2} \quad (eV^{-1}.cm^{-3}) \tag{4.11}$$

Substituting the values in the above equation number and considering that the Boltzmann Approximation is valid, the above equation (4.10) becomes

$$r_{sp}(\varepsilon) = \frac{m_r}{\pi\hbar^2 L_z \tau_r} f_n(\varepsilon_2)\left[1 - f_p(\varepsilon_1)\right] \quad (s^{-1}(eV)^{-1}cm^{-3}) \tag{4.12}$$

$$r_{sp}(\varepsilon) = \frac{(2m_r)^{3/2}}{2\pi\hbar^3\tau_r}\left(\varepsilon - \varepsilon_g\right)^{1/2} e^{(\varepsilon_{fn} - \varepsilon_{fp} - \varepsilon_g)} e^{-\left(\frac{\varepsilon - \varepsilon_g}{k_B T}\right)} (s^{-1}(eV)^{-1}cm^{-3}) \tag{4.13}$$

where $\varepsilon_{fn}, \varepsilon_{fp}$ are quasi fermi levels for electrons and holes respectively and ε_g is the bandgap of active region of the laser.

For a degenerate semiconductor, the qausi fermi levels can be related to carrier concentration using Joyce-Dixon approximation:

$$\varepsilon_{fn} = KT\left[ln\left(\frac{n}{N_C}\right) + \frac{1}{\sqrt{8}}\left(\frac{n}{N_C}\right)\right] \tag{4.14}$$

$$\varepsilon_{fp} = KT\left[ln\left(\frac{p}{N_V}\right) + \frac{1}{\sqrt{8}}\left(\frac{p}{N_V}\right)\right] \tag{4.15}$$

where n and p are the concentration of electron and holes in the conduction and valence band respectively. N_C and N_V are the effective density of states function in the conduction and valence band of the active region material. N_C and N_V depends on the type of material used and changes from material to material. For double heterojunction laser discussed in this chapter, the active region is made of GaAs for which $N_C = 4.7 * 10^{17}\ cm^{-3}$ and $N_V = 7 * 10^{18}\ cm^{-3}$ for GaAs [36].

Plotting the spontaneous emission rate for Double Heterojunction, we get the following graph:

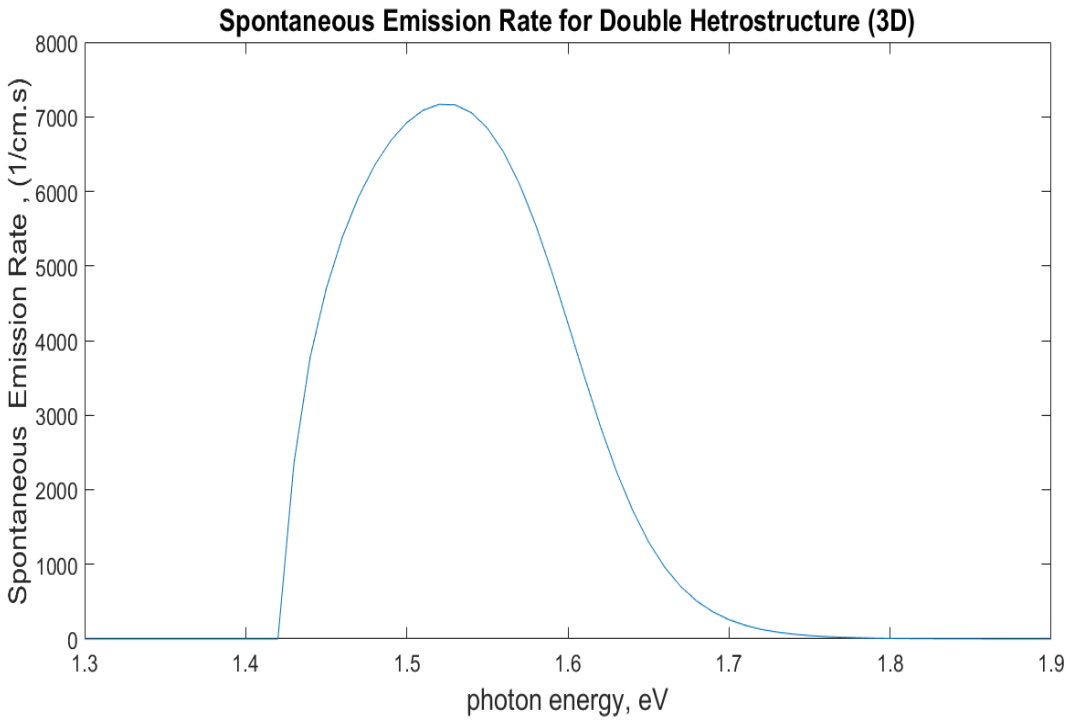

Figure. 4-5. Spontaneous Emission Spectra of Double Heterojunction Laser

The above graph represents the spontaneous emission spectra, and the shape of the graph is described by the linewidth function which defines that the given transition between conduction and valence band will result in absorption and emission of photon.

The total spontaneous emission rate per unit volume is defined as [24]:

$$R_{sp} = \int_{\varepsilon} r_{sp}(\varepsilon)\, d\varepsilon \quad (s^{-1}cm^{-3}) \tag{4.16}$$

Total spontaneous emission rate is an important parameter in laser design as it is used to find the emission coupling factor and threshold injection current of a semiconductor laser.

4.5. Stimulated Emission Rate

Stimulated Emission is the process by which an electron in the excited state is dropped to the ground state when it interacts with the incoming photon. The rate at which this process takes place is called stimulated emission rate. The stimulated emission rate per unit per energy interval is expresses as [25]:

$$r_{sti}^{3D} = \left(\frac{n_r^2\omega^2}{\pi^2\hbar c^2}\right) C_0 \frac{2}{V}\sum_{k_v}\sum_{k_c}|\hat{e}.p_{CV}|^2\,\delta(E_c - E_v - \hbar\omega)(f_c - f_v) \tag{4.17}$$

where n_r is the refractive index of the active material ,ω is the angular frequency, ħ is the reduced Planck's constant, $\frac{2}{V}\sum_{k_v}\sum_{k_c}$ are summations over all k vectors in valence and conduction bands respectively and represents the JODS , $|\hat{e}.p_{CV}|^2$ is the momentum matrix element and δ function is the kronecker delta and f_c and f_v is the occupation probability in conduction and valence band and $C_0$is a constant given by

$$C_0 = \frac{\pi e^2}{n_r c\varepsilon_0 m_{0\omega}^2} \tag{4.18}$$

Substituting the value of JODS in equation (4.16) the stimulated emission rate for a bulk semiconductor can be expressed as:

$$r_{3D}^{sti} = \left(\frac{n_r\omega e^2(1+\mu_\varepsilon)}{3\pi\hbar c^3\varepsilon_0 m_0^2}\right)|\hat{e}.p_{cv}|^2 f_c(1-f_v)\frac{(2m_r^*)^{3/2}}{2\pi^2\hbar^3} \tag{4.19}$$

4.6. Threshold Gain

The power gained by the waveguide mode from the active region is equal to the power drained from the waveguide mode by the passive regions of the guide. Taking cavity losses and mirror reflectivity into account we get,

$$\Gamma\, g_{th} = \left[\gamma + \frac{1}{2l} ln\left(\frac{1}{R_1R_2}\right)\right] \tag{4.20}$$

The above equation represents the threshold condition of the cavity. Gain is proportional to the injected carrier concentration n and the value at which gain is equal to $\left[\gamma + \frac{1}{2l} ln\left(\frac{1}{R_1 R_2}\right)\right]$, is known as the threshold carrier concentration n_{th} and the threshold gain the value of optical gain at which the round-trip gain is equal to the round-trip loss and hen the lasing occurs

The gain threshold is given by [24]:

$$g_{th} = \frac{1}{\Gamma}\left[\gamma + \frac{1}{2l} ln\left(\frac{1}{R_1 R_2}\right)\right] \tag{4.20}$$

where Γ is the optical confinement factor and is equal to 1, γ is the losses and l is the length of the cavity and $R_1\ and\ R_2$ are the reflectivities. From section 4.2, we get the optical confinement factor equal to 1, for GaAs the mirror reflectivities are given by 0.32. Taking, γ=10 cm^{-1} and l=400 μm and substituting these values in equation (4.20) we get $g_{th} = 38\ cm^{-1}$.

4.7. Conclusion

From the discussion in this chapter, it was found that gain is of the order of thousand which is higher than conventional laser made of other materials. The optical gain increases as we increase the carrier concentration and the linewidth was found to be broad in optical gain and spontaneous emission spectra of DH laser.

CHAPTER 5

MULTIPLE QUANTUM WELL LASER

5.1. Introduction

Quantum Well lasers have a narrow active region, due to which quantum confinement of charge carriers occurs and thus they are considered as reduced dimensional devices. The efficiency of quantum well laser is greater than bulk or conventional lasers due to quantum confinement. For compensation in the reduction of the active layers, identical quantum wells are used for the design, which is known as multiple quantum well (MQW) laser. In this chapter, we consider a MWQ structure which consists of 50 QW made of GaAs, with each QW sandwiched between barrier layer made of AlGaAs. The width the Quantum well and barrier layer is 10 nm. The structure of the MQW is explained by Figure 5-1.

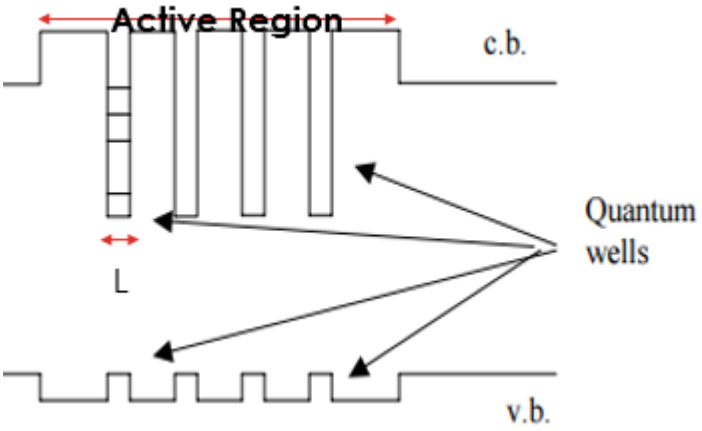

Figure. 5-1. Structure of the Multiple Quantum Well Laser

In Figure 5-1, v.b and c.b stands for valence band and conduction band respectively and L is the width of the quantum well.

Due to step density of states functions and Quantum confinement, MQW Well lasers exhibit large gain and spontaneous emission rate as compared to conventional Double Heterojunction lasers

which will be shown in this chapter. Also, the threshold injection current is low as compared to the laser discussed in previous chapter as the transparency carrier concentration for MQW laser is low as compared to the conventional lasers.

5.2. Optical Confinement Factor

Optical confinement factor of MQW Laser depends on the thickness and number of Quantum wells and barriers layers in the active region of the laser. The optical confinement factor of MQW Laser is given by [38]:

$$\Gamma = \frac{\gamma N_a t_a}{t} \tag{5.1}$$

where t is the thickness of the active region and N_a is the number of quantum wells and t_a is the thickness of quantum well, $\gamma = 0.95$ [38]. For the proposed design, $N_a = 50$ and $t_a = 10\ nm$. Calculating with the above relation Γ = 0.47.

5.3. Gain in the active region

Optical gain in a laser is equal to the net stimulated emission rate divided by the photon flux. This can be written as [24]:

$$g(\varepsilon) = \frac{power\ emitted\ per\ unit\ volume}{power\ crossing\ per\ unit\ area} \tag{5.2}$$

In other words,

$$g(\varepsilon) = \frac{r_{st}^{net}(\varepsilon)}{\frac{c.n_\varepsilon u_\varepsilon}{n_r}} \quad (cm)^{-1} \tag{5.3}$$

where n_ε is the photon mode density, u_ε is the photon occupation number, c is the speed of light and n_r is the refractive index of active material. In the above equation $r_{st}^{net}(\varepsilon)$ is given by [24]:

$$r_{st}^{net}(\varepsilon) = \frac{n_r\, q^2 \varepsilon\, p_{cv}^2 u_\varepsilon}{3\pi \epsilon_0 m_0^2 \hbar^2 c^3} N_J(\varepsilon)[f_n(\varepsilon_2) - f_p(\varepsilon_1)] \tag{5.4}$$

where $N_J(\varepsilon)$ is the Joint optical density of states, p_{cv}^2 is the oscillator strength.

For a Multiple Quantum, well laser the joint optical density of states is given by [39]:

$$N_J(\varepsilon) = \frac{N.m_r}{\pi \hbar^2 L_z} \tag{5.5}$$

where N is the number of quantum wells and m_r is the reduced effective mass and L_z is the width of the quantum well. For the proposed design, N=50 and $L_z = 10\ nm$.

To design a laser, it is essential to visualize the gain spectra of the given laser. For a multiple Quantum well laser the gain spectra can be obtained by substituting equation (5.5) and (5.4) in equation (5.3):

$$g(\varepsilon) = \frac{N.q^2 p_{cv}^2}{3\epsilon_0 m_0^2 c n_r\, \varepsilon} \frac{m_r}{\hbar L_z} [f_n(\varepsilon_2) - f_p(\varepsilon_1)] \tag{5.6}$$

Plotting the above relation, we get the following graph:

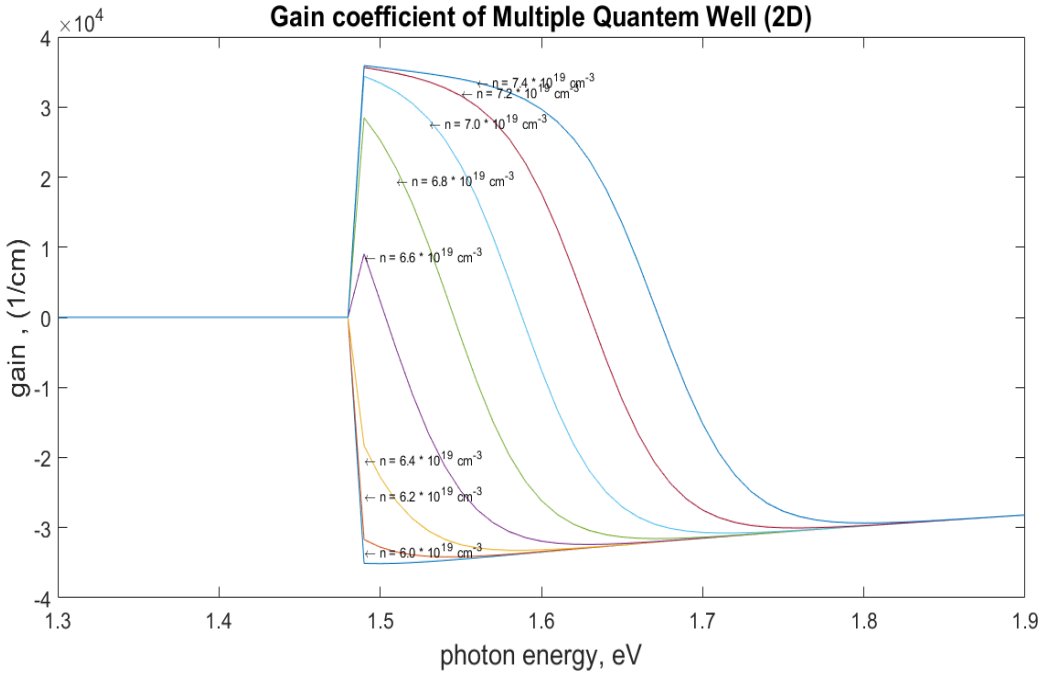

Figure. 5-2. Gain spectra of Multiple Quantum Well Laser

5.4. Comparison of DH laser and MQW laser optical gain

In this section, we will compare the optical gain of the Double Heterostructure discussed in chapter 4. We want to see the effect of dimensionality on the gain of these devices. The width of the active region is same in both devices, i.e. 1 micrometer. This section will explain the difference in the gain spectra of these devices even if the active region dimensions are the same. The difference in the structure can be observed by figure. 5-3.

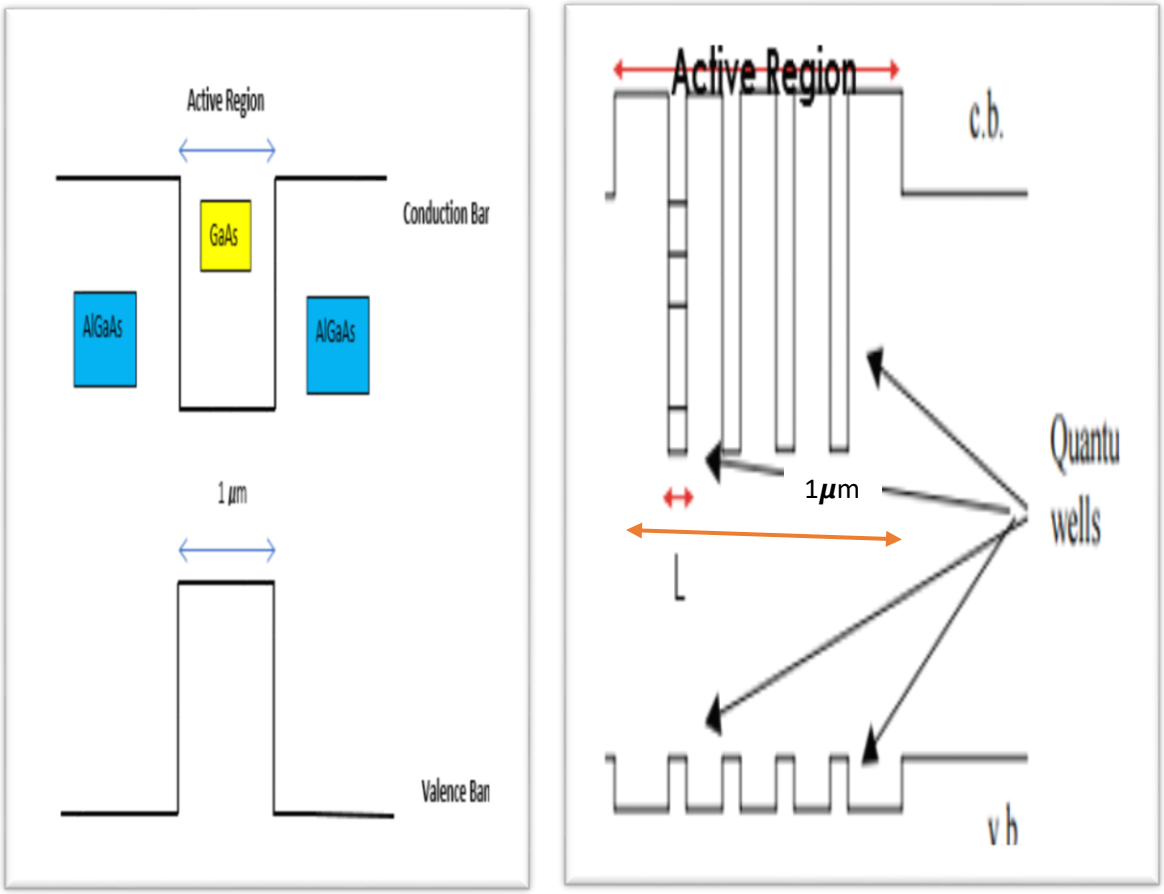

Figure. 5-3. Structure of DH laser (left) and MQW laser (right)

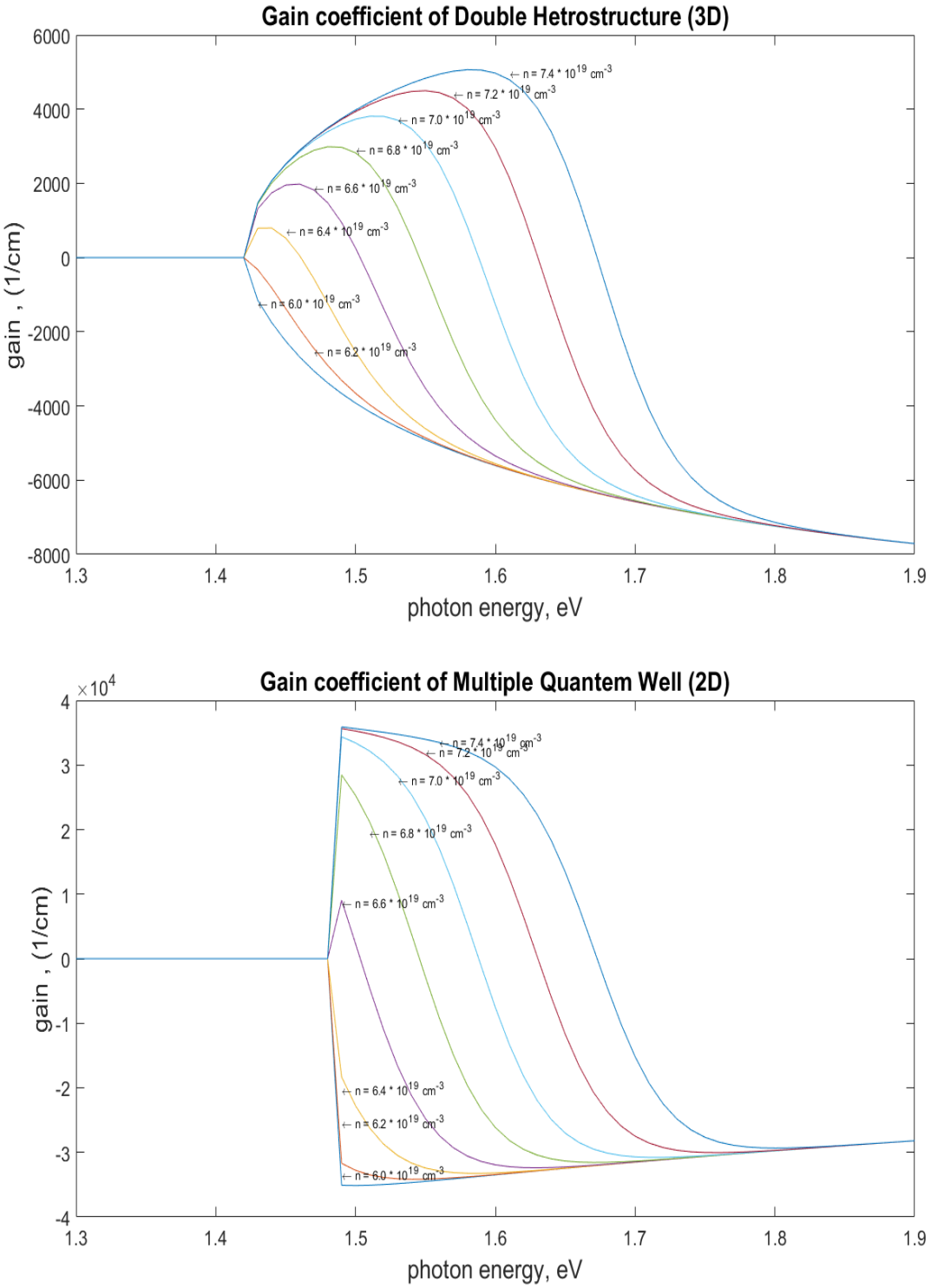

Figure. 5.4. Optical Gain of DH Laser (top) and MQW Laser (bottom)

As it can be seen in Figure 5-4 that the optical gain increases significantly for a MQW laser as compared to DH laser by a factor of 100. It is also observed that the optical gain increases with increase in carrier concentration. At energies, much larger than the band gap, the occupation of electrons and holes in the conduction band and valence band respectively is negligible and absorption process dominates. The gain is large in MQW as it shows dependence on JODS and JODS is large for MQW structures as compared to DH structures.

5.5. Spontaneous Emission Rate

As previously mentioned, the spontaneous emission rate for a laser is given by [24]:

$$r_{sp}(\varepsilon) = P_{em}\, N_J(\varepsilon) f_n(\varepsilon_2)\left[1 - f_p(\varepsilon_1)\right] \quad (s^{-1}(eV)^{-1}cm^{-3}) \tag{5.7}$$

where P_{em} is the emission probability, given by (see Appendix1):

$$\frac{n_r q^2 \varepsilon p_{cv}^2 (1 + u_\varepsilon)}{3\pi\varepsilon_0 m_o^2 \hbar^2 c^3}$$

When Boltzmann approximation is valid, $r_{sp}(\varepsilon)$ is given as:

$$r_{sp}(\varepsilon) = \frac{N_r m_r}{\pi\hbar^2 L_z \tau_r} e^{(\varepsilon_{fn} - \varepsilon_{fp} - \varepsilon_g)} e^{\left(-\frac{\varepsilon - \varepsilon_g}{K_B T}\right)} \ (s^{-1}eV^{-1}cm^{-3}) \tag{5.8}$$

where ε_{fn} and ε_{fp} are the quasi fermi levels which are given by Joyce Dixon approximation as follows:

$$\varepsilon_{fn} = KT\left[ln\left(\frac{n}{N_C}\right) + \frac{1}{\sqrt{8}}\left(\frac{n}{N_C}\right)\right] \tag{5.9}$$

$$\varepsilon_{fp} = KT\left[ln\left(\frac{p}{N_V}\right) + \frac{1}{\sqrt{8}}\left(\frac{p}{N_V}\right)\right] \tag{5.10}$$

Plotting the spontaneous emission rate for Multiple Quantum well laser, we get the following graph:

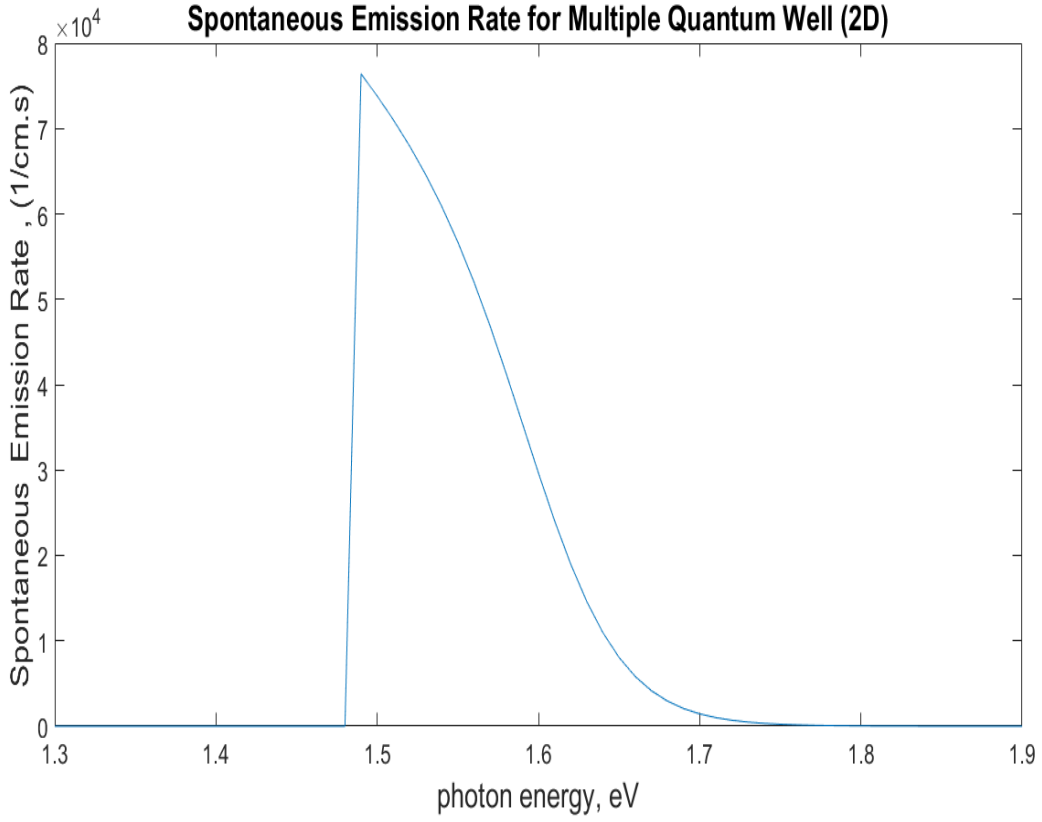

Figure. 5-5. Spontaneous Emission Spectra Multiple Quantum Well Laser

5.6. Comparison of DH laser and MQW laser Spontaneous Emission rate

In this section, we will compare the spontaneous emission rate for a DH and MWQ laser and analyze the reason for change in spontaneous emission rate for both the lasers. It can be seen from Table. 5-1 that the spontaneous emission rate depends on JODS for DH and MWQ lasers and JODS changes when we go from DH to MQW lasers due to reduced dimensionality.

	DH Laser	MQW Laser
Spontaneous Emission rate $(s^{-1}(eV)^{-1}cm^{-3})$	$P_{em}\, N_J(\varepsilon) f_n(\varepsilon_2)\left[1 - f_p(\varepsilon_1)\right]$	$P_{em}\, N_J(\varepsilon) f_n(\varepsilon_2)\left[1 - f_p(\varepsilon_1)\right]$
JODS $(eV^{-1}.cm^{-3})$	$N_J(\varepsilon) = \frac{(2m_r)^{3/2}}{2\pi\hbar^3}\left(\varepsilon - \varepsilon_g\right)^{1/2}$	$N_J(\varepsilon) = \frac{N.m_r}{\pi\hbar^2 L_z}$

Table 5-1. Spontaneous Emission rates for DH and MQW Laser

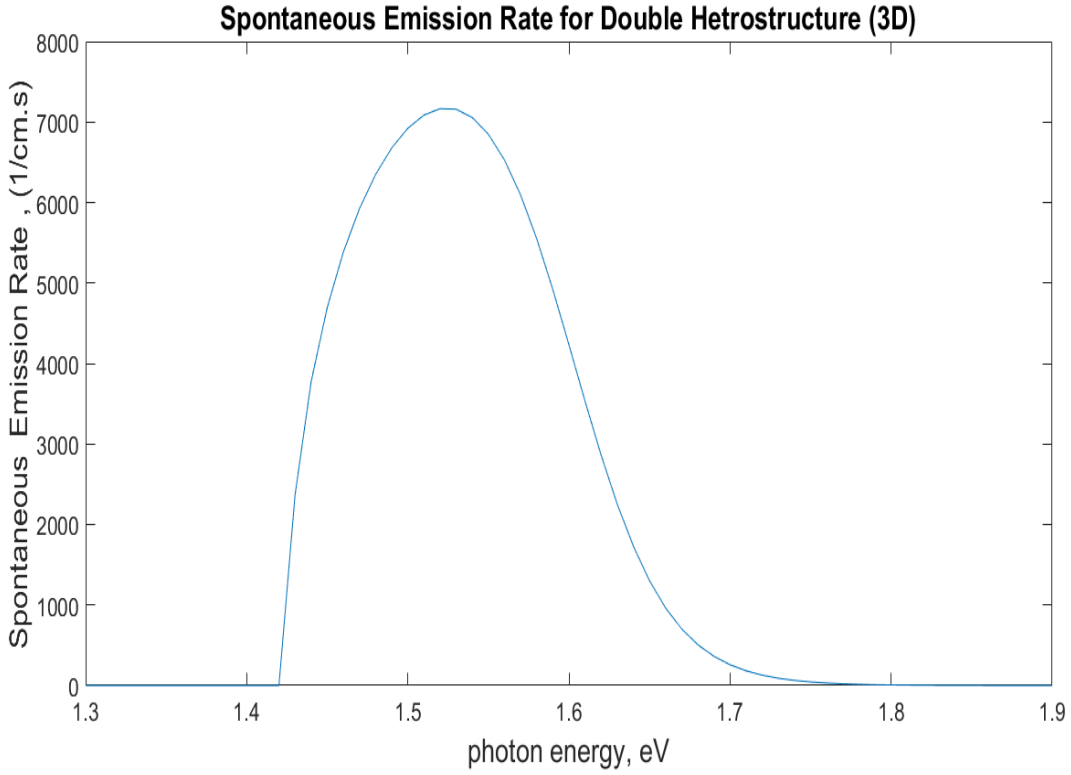

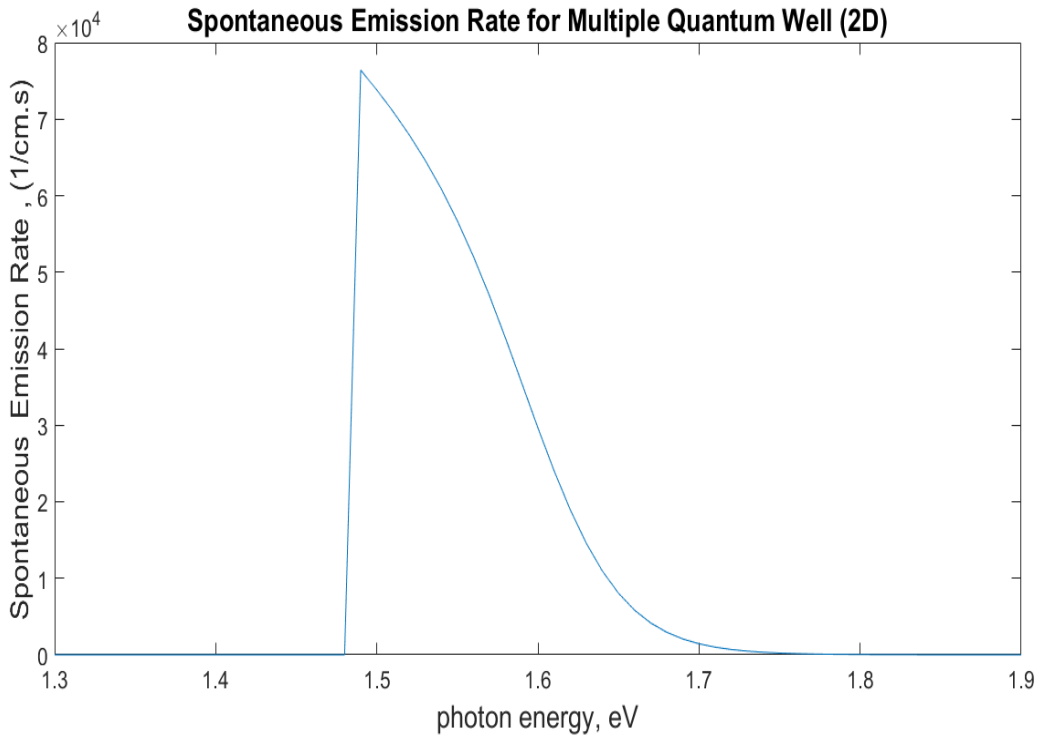

Figure. 5-6. Spontaneous Emission Spectra for DH laser (top) and MQW laser (bottom)

It can be seen from the Figure 5-5 that the spontaneous emission rate increases significantly for a MQW laser as compared to DH laser, due to its dependence on JODS (refer Table 1), which increases on moving from DH (3-D) to MWQ (2-D).

5.7. Threshold Gain

The power gained by the waveguide mode from the active region is equal to the power drained from the waveguide mode by the passive regions of the guide. Taking cavity losses and mirror reflectivity into account we get,

$$\Gamma\, g_{th} = \left[\gamma + \frac{1}{2l} ln\left(\frac{1}{R_1 R_2}\right)\right] \tag{5.11}$$

The above equation represents the threshold condition of the cavity. Gain is proportional to the injected carrier concentration n and the value at which gain is equal to $\left[\gamma + \frac{1}{2l} ln\left(\frac{1}{R_1 R_2}\right)\right]$, is known

as the threshold carrier concentration n_{th} and the thrshod gain the value of optical gain at which the round-trip gain is equal to the round-trip loss and hen the lasing occurs.

The gain threshold is given by [24]:

$$g_{th} = \frac{1}{\Gamma}\left[\gamma + \frac{1}{2l} ln\left(\frac{1}{R_1 R_2}\right)\right] \tag{5.12}$$

where Γ is the optical confinement factor and is equal to 0.47, γ is the losses and l is the length of the cavity and R_1 and R_2 are the reflectivities of the end facets. Taking γ, l , R_1 and R_2 same as taken for a Double Heterojunction Laser in chapter 5, we get g_{th}= 10 cm^{-1} by substituting the values in equation (5.12). When we compare the values of g_{th} for Double Heterojunction and MQW laser, we observe that the threshold gain reduces in MWQ lasers by a factor of 3.8 as compared to DH lasers.

5.8. Conclusion

From the discussion in this chapter it was found that the gain and spontaneous emission rate in MQW well laser was very high as compared to the Double Heterojunction Laser as discussed in chapter 4. In conclusion, the spontaneous emission rate and gain of MQW laser is high as compared to DH laser of the same active region width.

CHAPTER -6

NANOWIRE LASERS

6.1 Introduction

Semiconductor nanowires have been a subject of great interest in past few decades due to their unique optical and optoelectronic properties. They have various applications in optoelectronic devices such as photodetectors, LED's, solar cells, and lasers. These miniaturized one-dimensional structures attracted interests of many scientists when they were found to exhibit lasing action. III-V wide gap semiconductors were found to be an optimum choice for lasers. The first lasing action in a nanowire was observed for a ZnO nanowire in 2001. In the domain of nanowire lasers, ZnO and GaN have gained popularity due to their unique threshold gain and threshold current densities values.

6.2 Absorption in GaAs nanowires

Absorption in nanowires increases due to its reduced dimensionality and increased Joint optical density of states. The absorption is more as compared to double heterostructures and quantum well due to reduction in reduced effective mass of nanowires.

The absorption in nanowires can be observed with absorption coefficient which is given by [25]:

$$\alpha_{1D} = C_0|\hat{e}.p_{cv}|^2(f_v - f_c)\frac{(m_r^*)^{3/2}}{\pi\hbar m_e^* L_x L_y}\frac{1}{\sqrt{(\hbar\omega - E_g)}} \quad (6.1)$$

where f_v and f_c are fermi Dirac distribution function in valence band and conduction band respectively, p_{cv} is the oscillator strength and m_r and m_r are the reduced effective and effective mass of electrons. L_x and L_y are the nanowire widths

6.3 Optical Gain in GaAs nanowires

The gain in a nanowire is given by

$$g(\varepsilon) = \frac{power\ emitted\ per\ unit\ volume}{power\ crossing\ per\ unit\ area}$$

In other words,

$$g(\varepsilon) = \frac{r_{st}^{net}(\varepsilon)}{\frac{c.n_\varepsilon u_\varepsilon}{n_r}} \quad (cm)^{-1} \tag{6.2}$$

where n_ε is the photon mode density, u_ε is the photon occupation number. In the above equation $r_{st}^{net}(\varepsilon)$ is given by [24]:

$$r_{st}^{net}(\varepsilon) = \frac{n_r\, q^2 \varepsilon\, p_{cv}^2 u_\varepsilon}{3\pi\epsilon_0 m_0^2 \hbar^2 c^3} N_J(\varepsilon)[f_n(\varepsilon_2) - f_p(\varepsilon_1)] \tag{6.3}$$

Here $f_n(\varepsilon_2)$ and $f_p(\varepsilon_1)$ distribution functions for electron and holes in conduction and valence band and are given by [24]:

$$f_p(\varepsilon_1) = exp\left(\frac{\varepsilon - \varepsilon_{fp}}{K_B T}\right) \tag{6.4}$$

$$f_n(\varepsilon_2) = exp\left(\frac{\varepsilon_{fn} - \varepsilon}{K_B T}\right) \tag{6.5}$$

where ε_{fp} and ε_{fn} are quasi fermi levels in valence and conduction band respectively.

$N_J(\varepsilon)$ in equation (6.3) is the Joint optical density of states for nanowire and is given by [25]:

$$N_J(\varepsilon) = \frac{1}{L_x L_y \pi}\sqrt{\frac{2m_r}{\hbar^2}}\ \frac{1}{\sqrt{\hbar\omega - E_{cv}^{mn}}} \quad (eV^{-1}.cm^{-3}) \tag{6.6}$$

where,

$$E_{cv}^{mn} = E_g + \frac{\hbar^2}{2m_r}\left[\left(\frac{m\pi}{a}\right)^2 + \left(\frac{n\pi}{b}\right)^2\right] \quad (6.7)$$

L_x and L_y is the width of the rectangular nanowire of cross section a and b.

Where E_g is the band gap and m_r is the reduced effective mass of nanowire,m and n are the quantum numbers in the valence and conduction band respectively, a and b are the width of the nanowire. The gain of the nanowire can be derived as:

$$g(\varepsilon) = \frac{n_r\, q^2 \varepsilon\, p_{cv}^2 u_\varepsilon}{L_x L_y 3\pi\epsilon_0 m_0^2 \hbar^2 c^3} \frac{1}{\pi}\sqrt{\frac{2m_r}{\hbar^2}} \quad \frac{1}{\sqrt{\hbar\omega - E_{cv}^{mn}}}[f_n(\varepsilon_2) - f_p(\varepsilon_1)] \quad (6.8)$$

Plotting the above relation, we get the gain spectrum of nanowire laser:

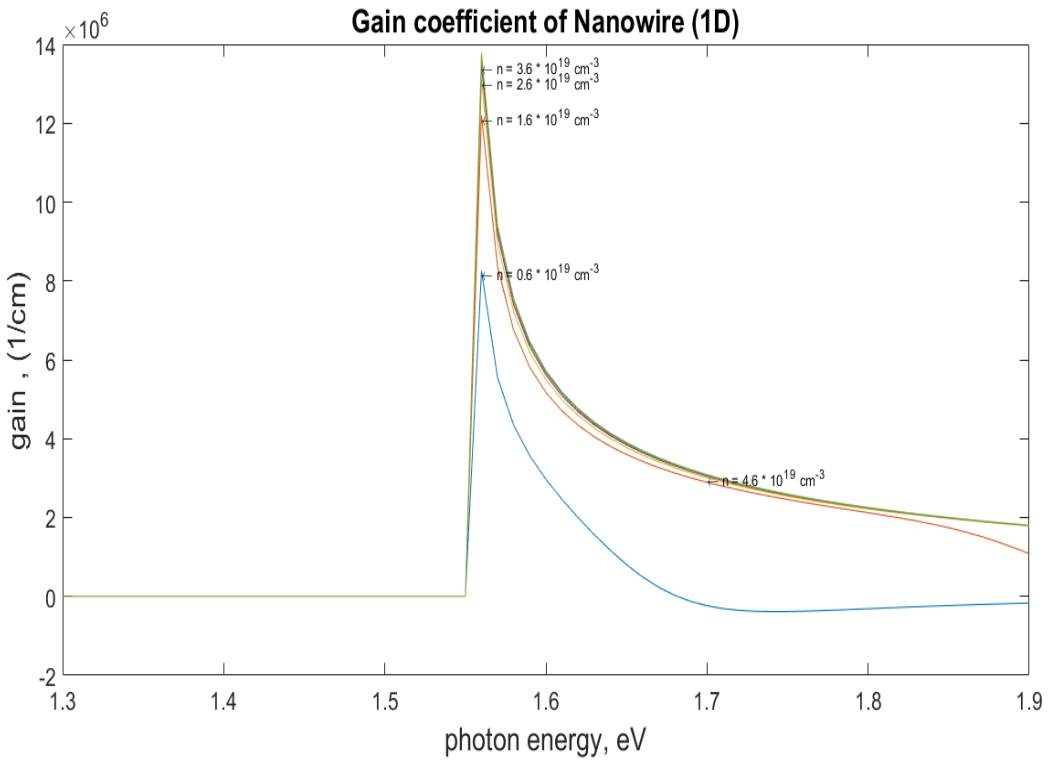

Figure. 6-1. Optical gain spectra of a Nanowire laser

From Figure. 6-1, It is seen that the linewidth of the spectrum decreases and the shape account for

the JODS of a nanowire. The optical gain increases as we increase the carrier concentration, n**.**

6.4. Comparison of optical gain of DH, MQW and Nanowire lasers

In this section, we will compare the optical gain in DH, MQW and Nanowire lasers. We observe the effect of dimensionality on the optical gain by generating the spectral response of gain of these devices. The effect of JODS on the optical gain on these devices is also explained**.**

	Optical Gain	**JODS**
Nanowire Laser	$g(\varepsilon) = \frac{n_r q^2 \varepsilon p_{cv}^2 u_\varepsilon}{L_x L_y 3\pi \in_0 m_0^2 \hbar^2 c^3} \frac{1}{\pi} \sqrt{\frac{2m_r}{\hbar^2}} \frac{1}{\sqrt{\hbar\omega - E_{cv}^{mn}}} [f_n(\varepsilon_2) - f_p(\varepsilon_1)]$	$N_J(\varepsilon) = \frac{1}{L_x L_y \pi} \sqrt{\frac{2m_r}{\hbar^2}} \frac{1}{\sqrt{\hbar\omega - E_{cv}^{mn}}}$ $(eV^{-1}.cm^{-3})$
MQW Laser	$g(\varepsilon) = \frac{N.q^2 p_{cv}^2}{3\epsilon_0 m_0^2 c n_r \varepsilon} \frac{m_r}{\hbar L_z} [f_n(\varepsilon_2) - f_p(\varepsilon_1)]$	$N_J(\varepsilon) = \frac{N.m_r}{\pi\hbar^2 L_z}$
DH Laser	$g(\varepsilon) = \frac{\sqrt{2}(m_r)^{3/2} q^2 p_{cv}^2}{3\pi n_r \epsilon_0 m_0^2 \hbar^2 c\varepsilon} (\varepsilon - \varepsilon_g)^{1/2} [f_n(\varepsilon_2) - f_p(\varepsilon_1)]$	$N_J(\varepsilon) = \frac{(2m_r)^{3/2}}{2\pi\hbar^3} (\varepsilon - \varepsilon_g)^{1/2}$ $(eV^{-1}.cm^{-3})$

Table. 6-1. Optical Gain for DH, MQW and Nanowire Laser

From Table 6-1 it can be deduced that is dependent on the occupation probability and JODS. The effect of JODS is explained by gain spectrum of DH, MQW and Nanowire laser shown in Figure 6-1.

Nanowire Laser	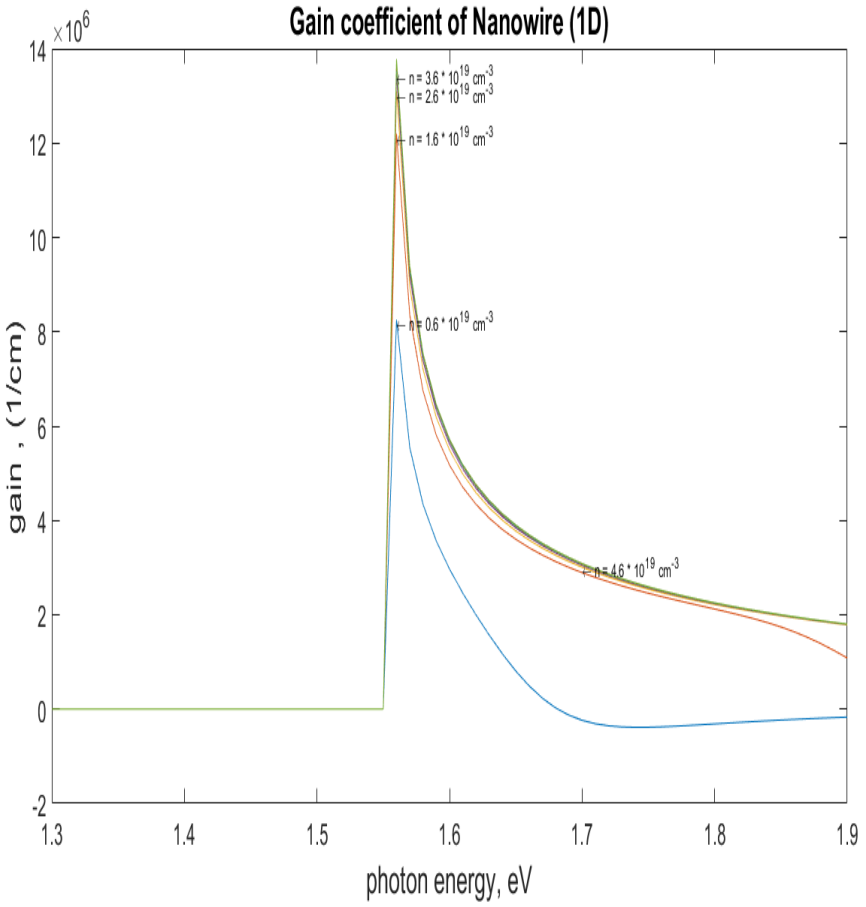

MQW laser	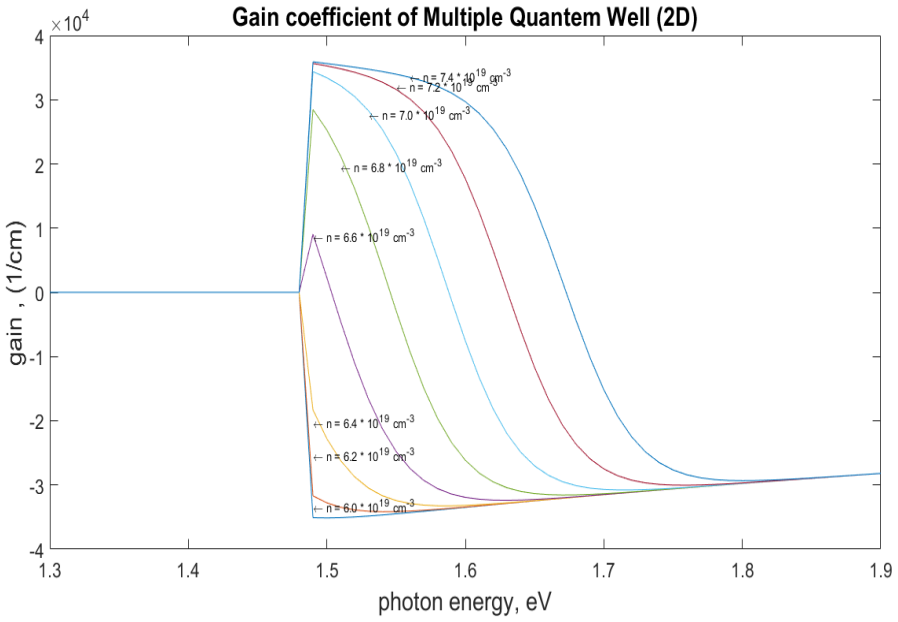
DH laser	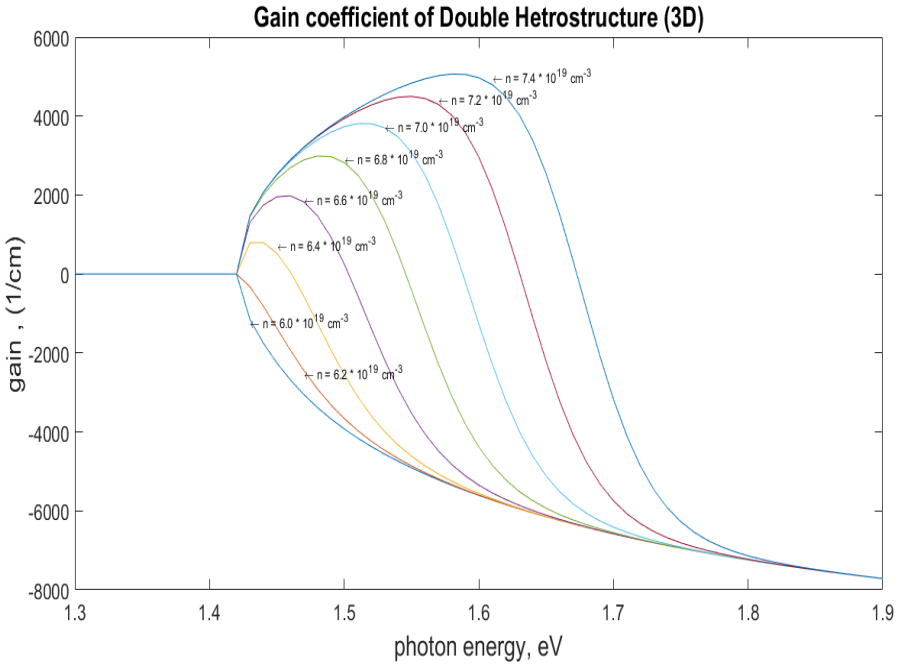

Figure. 6-2. Optical gain spectra for DH, MQW and Nanowire lasers

It can be seen from Figure 6-1. That the value of gain increases from DH laser to MQW lasers to Nanowire lasers due to the increase in JODS as the dimension decreases from DH to Nanowire lasers.

6.5 Stimulated Emission rate in GaAs nanowires

Stimulated emission is the process where the atom in the higher energy states drops to a lower energy state when a photon is incident on a two-level semiconductor system. Stimulated emission rates are enhanced in nanowires as compared to double heterostructure and quantum wells due to reduction in reduced effective mass and increase in Joint Optical Density of stages. The stimulated emission rates in a nanowire is given by [25]:

$$r_{ID}^{sti} = \left(\frac{n_r \omega e^2 (1+\mu_\varepsilon)}{\pi \hbar c^3 \varepsilon_0 m_0^2}\right) |\hat{e}.p_{cv}|^2 f_c(1-f_v) \frac{(m_r^*)^{3/2}}{\pi \hbar m_e^* L_x L_y} \tag{6.9}$$

6.6 Spontaneous Emission rate in GaAs nanowires

The spontaneous emission rate for a laser is given by [24]:

$$r_{sp}(\varepsilon) = P_{em}\, N_J(\varepsilon) f_n(\varepsilon_2)\left[1 - f_p(\varepsilon_1)\right] \quad (s^{-1}(eV)^{-1}cm^{-3}) \tag{6.10}$$

where $P_{em} = \frac{n_r q^2 \varepsilon p_{cv}^2 (1+u_\varepsilon)}{3\pi\varepsilon_0 m_0^2 \hbar^2 c^3}$ known as the probability of emission (refer Appendix 1).

When Boltzmann approximation is valid, $r_{sp}(\varepsilon)$ is given as:

$$r_{sp}(\varepsilon) = \frac{n_r q^2 \varepsilon p_{cv}^2 (1+u_\varepsilon)}{L_x L_y 3\pi\varepsilon_0 m_0^2 \hbar^2 c^3} \frac{1}{\pi} \sqrt{\frac{2m_r}{\hbar^2}} \; \frac{1}{\sqrt{\hbar\omega - E_{cv}^{mn}}} e^{(\varepsilon_{fn} - \varepsilon_{fp} - \varepsilon_g)} e^{\left(-\frac{\varepsilon - \varepsilon_g}{K_B T}\right)} \; (s^{-1}eV^{-1}cm^{-3}) \tag{6.11}$$

where ε_{fn} and ε_{fp} are the quasi fermi levels which are given by Joyce Dixon approximation as follows:

$$\varepsilon_{fn} = KT\left[ln\left(\frac{n}{N_C}\right) + \frac{1}{\sqrt{8}}\left(\frac{n}{N_C}\right)\right] \quad (6.12)$$

$$\varepsilon_{fp} = KT\left[ln\left(\frac{p}{N_V}\right) + \frac{1}{\sqrt{8}}\left(\frac{p}{N_V}\right)\right] \quad (6.13)$$

Plotting the spontaneous emission rate for Multiple Quantum well laser, we get the following graph:

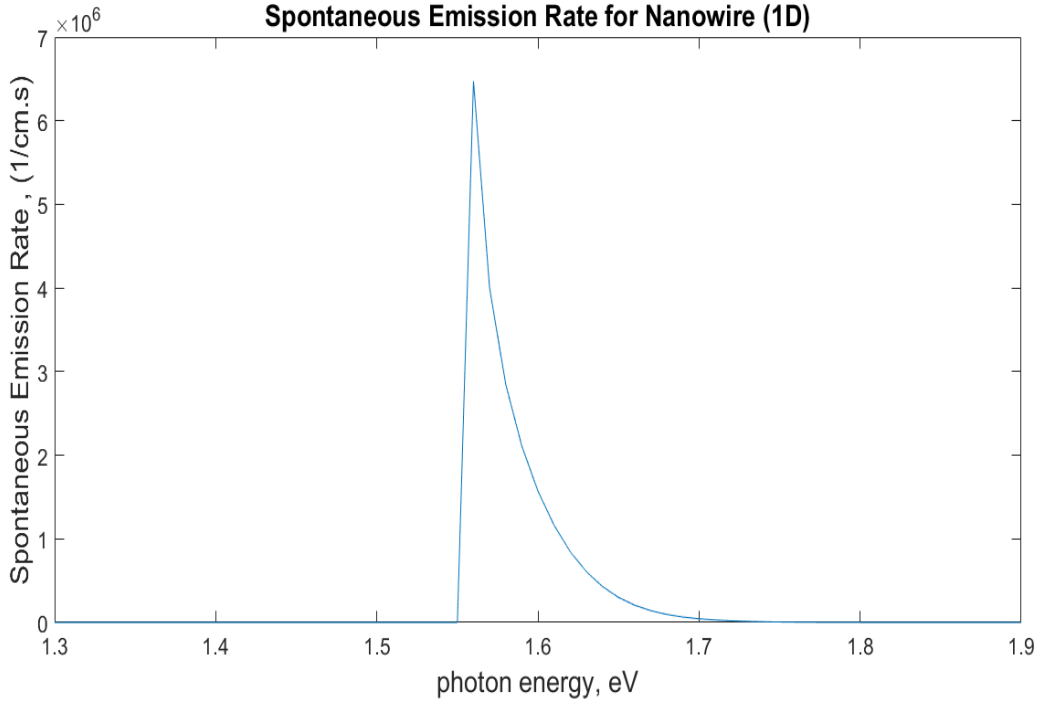

Figure. 6-3. Spontaneous Emission spectra of Nanowire Laser

6.7. Comparison of Spontaneous Emission Rate of DH laser, MWQ laser and Nanowire laser

In this section, we compare the spontaneous emission rate of DH, MQW and Nanowire lasers. Table 6-2 signifies the role of JODS in the spontaneous emission rate of these devices.

	DH Laser	MQW Laser	Nanowire Laser
Spontaneous Emission Rate $(s^{-1}eV^{-1}cm^{-3})$	$P_{em}\, N_J(\varepsilon) f_n(\varepsilon_2)\left[1 - f_p(\varepsilon_1)\right]$	$P_{em}\, N_J(\varepsilon) f_n(\varepsilon_2)\left[1 - f_p(\varepsilon_1)\right]$	$r_{sp}(\varepsilon) = \frac{1}{\pi}\sqrt{\frac{2m_r}{\hbar^2}} \frac{1}{\sqrt{\hbar\omega - E_{cv}^{mn}}} e^{(\varepsilon_{fn} - \varepsilon_{fp} - \varepsilon_g)} e^{\left(-\frac{\varepsilon - \varepsilon_g}{K_B T}\right)}$
JODS $(eV^{-1}.cm^{-3})$	$N_J(\varepsilon) = \frac{(2m_r)^{3/2}}{2\pi\hbar^3}(\varepsilon - \varepsilon_g)^{1/2}$	$N_J(\varepsilon) = \frac{N.m_r}{\pi\hbar^2 L_z}$	$N_J(\varepsilon) = \frac{1}{\pi L_x L_y}\sqrt{\frac{2m_r}{\hbar^2}} \frac{1}{\sqrt{\hbar\omega - E_{cv}^{mn}}}$ $(eV^{-1}.cm^{-3})$ where, $E_{cv}^{mn} = E_g + \frac{\hbar^2}{2m_r}\left[\left(\frac{m\pi}{a}\right)^2 + \left(\frac{n\pi}{b}\right)^2\right]$

Table. 6-2. Spontaneous Emission rate of DH, MQW and Nanowire lasers

From Table. 6-2., the spontaneous emission rate of DH, MQW and Nanowire lasers depend on the Joint Optical Density of states.

Nanowire Laser	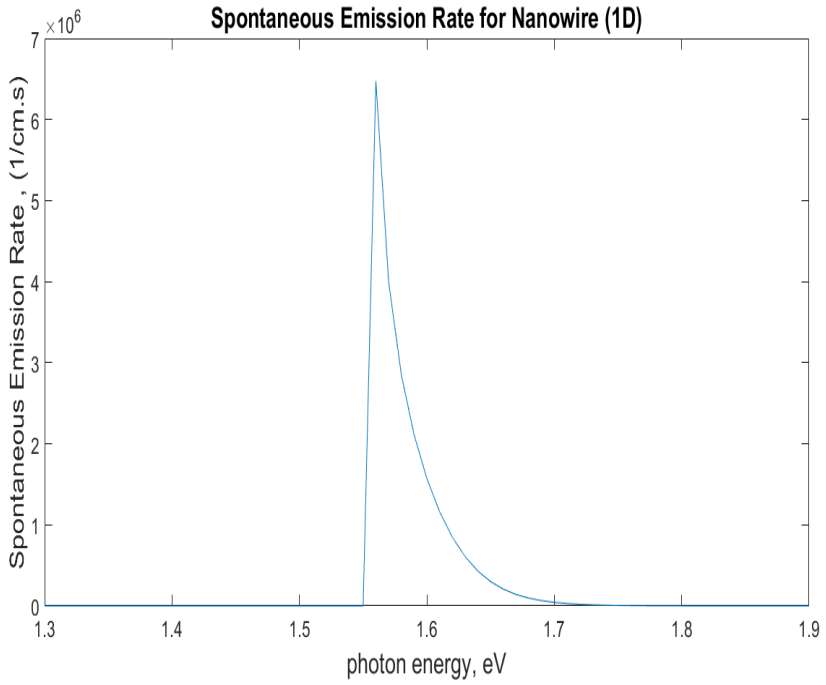
MQW laser	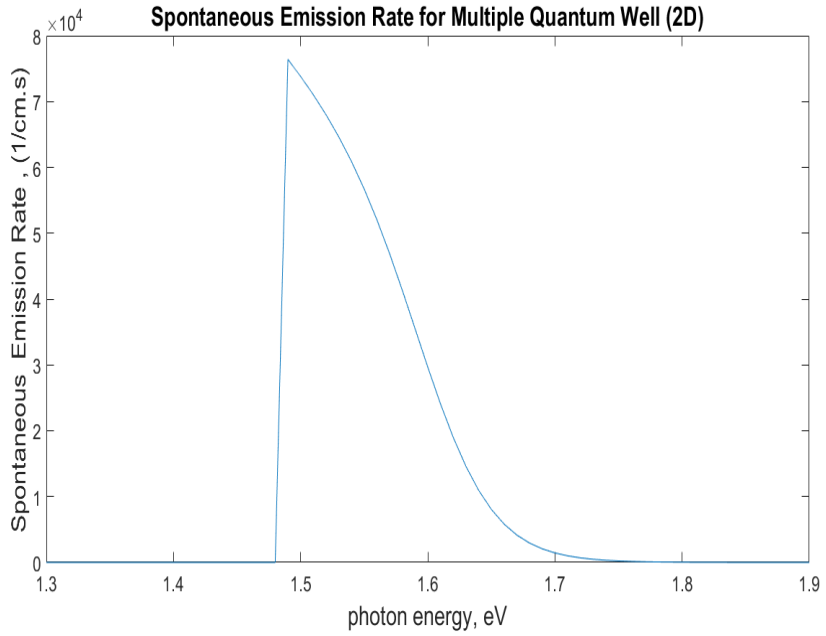

DH laser	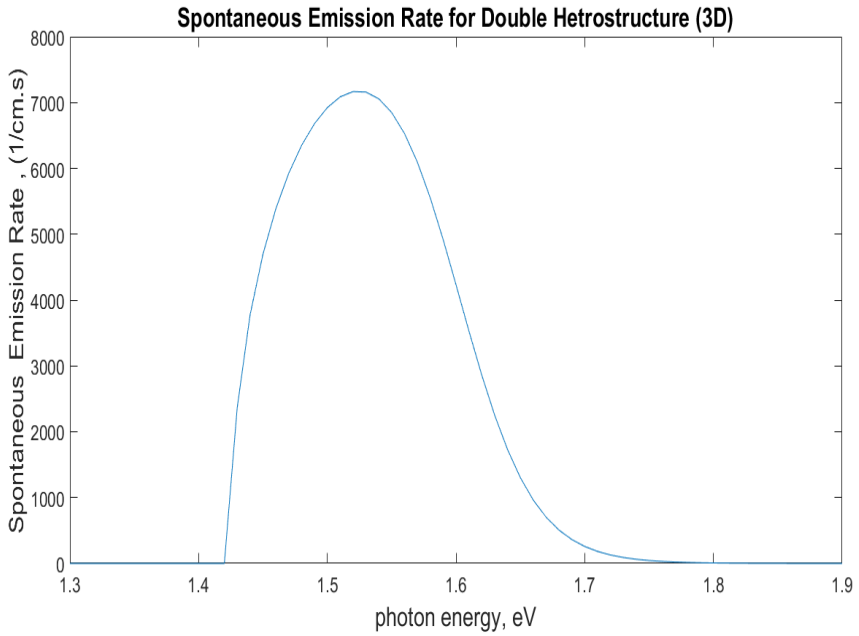

Figure. 6-4. Spontaneous Emission spectra for DH, MQW and Nanowire Lasers

From Figure. 6-3., it can be seen that the spontaneous emission rates increase significantly when we move from DH laser to MQW laser to QW lasers. This is due the dependence on the JODS which increases as we reduce the dimensions of a device and move from 3D to 1D.

6.8. Conclusion

In this chapter, we derive and examine the spontaneous emission rate and gain of nanowire lasers. Also, we compare this with the MQW laser and DH laser explained in chapter 4 and 5. It can be seen that the spontaneous emission rate and optical gain increases as we reduce device dimensions, i.e. from 3D to 1D device.

SUMMARY AND CONCLUSION

In this thesis, we study the effects of dimensionality on transition rates and gain in optoelectronic devices. Here we examine the change in the device optoelectronics properties due to change in dimensional dependent parameters. We see that the JODS is a significant parameter which changes as we reduce the dimension of an optoelectronic device and becomes large as the dimensions of the device decreases. It was also observed that oscillator strength plays an important role on transition rates in DH, MQW and nanowire lasers as oscillator strength increases as we move from DH (3-D), MQW (2-D) and nanowire lasers (1-D). In this thesis, we derived, examined, and analyzed the spontaneous emission rate and optical gain of DH, MQW and nanowire lasers. It was observed that the gain and spontaneous emission rate was dependent on JODS and oscillator strength which are dimensional dependent parameters. It can be seen in chapter 6 that the gain and spontaneous emission rates increased as the device dimensions decreased, i.e. from DH to nanowire lasers. The change in the shape of the peaks of the gain and spontaneous emission rate was attributed to the JODS which changed from 3D to 1D devices. It was also observed that the gain in each device increased as the injected carrier concentration increased. This was due to the Fermi Dirac distribution, which shows dependence on quasi fermi levels which are a factor of injected carrier concentration. From the comparison of optical gain and spontaneous emission rate in chapter 6, it can be seen that the gain and spontaneous emission rate in MWQ (2D) lasers increases by a factor of 10 as compared to DH (3D) lasers and in nanowire (1D) lasers it increases by a factor of 100 as compared to MQW lasers and by a factor of 1000 as compared to DH lasers. From the above discussion and analysis, it can be concluded that the efficiency of devices increases as the device dimensions reduces.

Bibliography

[1] Kroemer, H. (1957). Theory of a wide-gap emitter for transistors. *Proceedings of the IRE*, *45*(11), 1535-1537.

[2] Alferov, Z. I. (2002). The double heterostructure: Concept and its applications in physics, electronics and technology. *International Journal of Modern Physics B*, *16*(05), 647-675.

[3] Alferov, Z. I., Andreev, V. M., Portnoi, E. L., & Trukan, M. K. (1970). AlAs-GaAs heterojunction injection lasers with a low room-temperature threshold. *Sov Phys Semiconductors*, *3*(9), 1107-1110.

[4] Alferov, Z. I., Andreev, V. M., Garbuzov, D. Z., Zhilyaev, Y. V., Morozov, E. P., Portnoi, E. L., & Trofim, V. G. (1971). Investigation of the influence of the AlAs-GaAs heterostructure parameters on the laser threshold current and the realization of continuous emission at room temperature. *Sov. Phys. Semicond*, *4*(9), 1573-1575.

[5] Van der Ziel, J. P., Dingle, R., Miller, R. C., Wiegmann, W., & Nordland Jr, W. A. (1975). Laser oscillation from quantum states in very thin GaAs− Al0. 2Ga0. 8As multilayer structures. *Applied Physics Letters*, *26*(8), 463-465.

[6] Dingle, R., Wiegmann, W., & Henry, C. H. (1974). Quantum states of confined carriers in very thin Al x Ga 1− x As-GaAs-Al x Ga 1− x As heterostructures. *Physical Review Letters*, *33*(14), 827.

[7] Schmitt-Rink, S., Chemla, D. S., & Miller, D. A. B. (1989). Linear and nonlinear optical properties of semiconductor quantum wells. *Advances in Physics*, *38*(2), 89-188.

[8] Haug, H. (Ed.). (2012). *Optical nonlinearities and instabilities in semiconductors*. Elsevier.

[9] Von Lehmen, A., Zucker, J. E., Heritage, J. P., Chemla, D. S., & Gossard, A. C. (1986). Two-wavelength absorption modulation spectroscopy of bandtail absorption in GaAs quantum wells. *Applied physics letters*, *48*(21), 1479-1481.

[10] Stradling, R. A. (1996). The electronic properties and applications of quantum wells and superlattices of III-V narrow gap semiconductors. *Brazilian Journal of Physics*, *26*, 7-20.

[11] Nagle, J., & Weisbuch, C. (1988). Design rules of quantum well lasers. *Journal of Luminescence*, *40*, 713-714.

[12] Tarucha, S., Horikoshi, Y., & Okamoto, H. (1983). Optical Absorption Characteristics of GaAs–AlGaAs Multi-Quantum-Well Heterostructure Waveguides. *Japanese Journal of Applied Physics*, *22*(8A), L482.

[13] Wang, J., Ren, X., Deng, C., Hu, H., He, Y., Cheng, Z., ... & Yan, X. (2015). Extremely Low-Threshold Current Density InGaAs/AlGaAs Quantum-Well Lasers on Silicon. *Journal of Lightwave Technology*, *33*(15), 3163-3169.

[14] She, C., Fedin, I., Dolzhnikov, D. S., Demortière, A., Schaller, R. D., Pelton, M., & Talapin, D. V. (2014). Low-threshold stimulated emission using colloidal quantum wells. *Nano letters*, *14*(5), 2772-2777.

[15] Kuo, J. M., Chen, Y. K., Wu, M. C., & Chin, M. A. (1991). InGaAs/GaAs/InGaP multiple-quantum-well lasers prepared by gas-source molecular beam epitaxy. *Applied physics letters*, *59*(22), 2781-2783

[16] Nagle, J., Hersee, S., Razeghi, M., Krakowski, M., De Cremoux, B., & Weisbuch, C. (1986). Properties of 2D quantum well lasers. *Surface Science*, *174*(1-3), 148-154.

[17] Duan, X., Wang, J., & Lieber, C. M. (2000). Synthesis and optical properties of gallium arsenide nanowires. *Applied Physics Letters*, *76*(9), 1116-1118.

[18] Soci, C., Zhang, A., Bao, X. Y., Kim, H., Lo, Y., & Wang, D. (2010). Nanowire photodetectors. *Journal of nanoscience and nanotechnology*, *10*(3), 1430-1449.

[19] Bao, J., Zimmler, M. A., Capasso, F., Wang, X., & Ren, Z. F. (2006). Broadband ZnO single-nanowire light-emitting diode. *Nano letters*, *6*(8), 1719-1722.

[20] Garnett, E. C., Brongersma, M. L., Cui, Y., & McGehee, M. D. (2011). Nanowire solar cells. *Annual Review of Materials Research*, *41*, 269-295.

[21] Huang, M. H., Mao, S., Feick, H., Yan, H., Wu, Y., Kind, H., ... & Yang, P. (2001). Room-temperature ultraviolet nanowire nanolasers. *science*, *292*(5523), 1897-1899.

[22] Saxena, D., Mokkapati, S., Tan, H. H., & Jagadish, C. (2012, December). Designing single GaAs nanowire lasers. In *Optoelectronic and Microelectronic Materials & Devices (COMMAD), 2012 Conference on* (pp. 101-102). IEEE.

[23] Gu, Z., Prete, P., Lovergine, N., & Nabet, B. (2011). On optical properties of GaAs and GaAs/AlGaAs core-shell periodic nanowire arrays. *Journal of Applied Physics*, *109*(6), 064314.

[24] Bhattacharya, P., & Pang, L. Y. (1994). Semiconductor optoelectronic devices.

[25]. Chuang, S. L. (2012). *Physics of photonic devices* (Vol. 80). John Wiley & Sons.

[26] Coldren, L. A., Corzine, S. W., & Mashanovitch, M. L. (2012). *Diode lasers and photonic integrated circuits* (Vol. 218). John Wiley & Sons.

[27] Chuang, S. L., & Chuang, S. L. (1995). Physics of optoelectronic devices.

[28] Singh, J. (2007). *Electronic and optoelectronic properties of semiconductor structures*. Cambridge University Press.

[29] Pierret, R. F. (1996). *Semiconductor device fundamentals*. Pearson Education India.

[30] Demtröder, W. (2013). *Laser spectroscopy: basic concepts and instrumentation*. Springer Science & Business Media.

[31] Robinson, J. W. (1996). *Atomic spectroscopy*. CRC Press.

[32] Hilborn, R. C. (1982). Einstein coefficients, cross sections, f values, dipole moments, and all that. *American Journal of Physics*, *50*(11), 982-986

[33]. Matsuura, M., & Kamizato, T. (1986). Oscillator strength of excitons in quantum wells. *Surface Science*, *174*(1), 183-187.

[34]. Suemune, I., & Coldren, L. A. (1988). Band-mixing effects and excitonic optical properties in GaAs quantum wire structures-comparison with the quantum wells. *Quantum Electronics, IEEE Journal of*, *24*(8), 1778-1790.

[35]. Suemune, I., Coldren, L. A., & Corzine, S. W. (1988). Polarization dependent absorption spectra in quantum wire structures. *Superlattices and Microstructures*, *4*(1), 19-22.

[36]. GaAs-Gallium arsenide. Basic parameter at 300K. Retrieved from: http://www.ioffe.ru/SVA/NSM/Semicond/GaAs/basic.html

[37] Neamen, D. (2002). *Semiconductor physics and devices*. McGraw-Hill, Inc.

[38] Streifer, W., Scifres, D. R., & Burnham, R. D. (1979). Optical analysis of multiple-quantum-well lasers. *Applied optics*, *18*(21), 3547-3548.

[39] Arakawa, Y., & Yariv, A. (1986). Quantum well lasers--Gain, spectra, dynamics. *IEEE journal of quantum electronics*, *22*(9), 1887-1899.

APPENDIX 1

Derivation of Emission Probability

In this section, we will derive the emission probability for a direct band transition from valence band to conduction band. We consider that the valence band is full and k' determines the momentum of transition which is the momentum of the charge carrier in the valence band and k' is the equal to k'' (momentum of charge carrier in conduction band minima). The transition probability for a transition between $\varepsilon_C(k')$ and $\varepsilon_V(k'')$ is given by:

$$|A_m|^2 = |A_k''|^2 \frac{4|H_{k''k'}|^2 sin^2[(\varepsilon_k'' - \varepsilon_k' - \hbar\omega)t/2\hbar]}{(\varepsilon_k'' - \varepsilon_k' - \hbar\omega)^2} \quad \text{(A1.1)}$$

The momentum matric element $H_{k''k'}$is given by

$$H_{k''k'} = -\frac{qA}{2m_0} a_0 . p_{cv} \quad \text{(A1.2)}$$

Transition probability can be defined as per unit volume per unit time. Combining equation (A1.1) and equation (A1.2), transition emission probability is given as:

$$P(\hbar\omega)t = \frac{1}{4\pi^3}|A_k''|^2 = \frac{q^2|A|^2}{4\pi^3 m_0^2} \int \frac{|a_0 . p_{cv}|^2 sin^2[(\varepsilon_k'' - \varepsilon_k' - \hbar\omega)t/2\hbar]k''^2 dk''}{(\varepsilon_k'' - \varepsilon_k' - \hbar\omega)^2} \quad \text{(A1.3)}$$

where dk'=$k'^2 dk' d\Omega$ and $d\Omega$=sin θ $d\phi$. And

$$\int |a_0 . p_{cv}|^2 d\Omega = 4\pi p_{cv}^2 \quad \text{(A1.4)}$$

Therefore,

$$P(\hbar\omega)t = \frac{q^2|A|^2}{m_0^2} \int \frac{p_{cv}^2 sin^2[(\varepsilon_k'' - \varepsilon_k' - \hbar\omega)t/2\hbar]k''^2 dk''}{(\varepsilon_k'' - \varepsilon_k' - \hbar\omega)^2} \quad \text{(A1.5)}$$

where

$$|A|^2 = \frac{u_\varepsilon \hbar}{2\varepsilon_0 \omega V} \tag{A1.6}$$

Taking $\varepsilon_k'' - \varepsilon_k' - \hbar\omega = x$ and substituting equation (A1.6) in (A1.5) we get

$$P_{em} = \frac{n_r q^2 \varepsilon p_{cv}^2 (1+u_\varepsilon)}{3\pi\varepsilon_0 m_o^2 \hbar^2 c^3} \tag{A1.7}$$

References:

[1] Bube, R. (2012). *Electronic properties of crystalline solids: an introduction to fundamentals*. Elsevier.

[2] Bhattacharya, P. (1994). *Semiconductor optoelectronic devices*. Prentice-Hall, Inc.